On the Microscale: Dorsal Snakeskin Microstructure Variation

By

Arin Rinvelt

A Paper Presented to the

Faculty of Mount Holyoke College in

Partial Fulfillment of the Requirements for

The Degree of Bachelors Arts with

Honor

Department of Biological Sciences

South Hadley, MA 01075

May 2024

This paper was prepared
under the direction of
Professor Patricia Brennan
for eight credits

ACKNOWLEDGMENTS

I would like to thank Professor Patrica Brennan for accepting me into her lab and giving me the opportunity to create my own thesis project. Despite my project being outside her realm of expertise, she was not afraid to learn all about snake microstructures with me. Thank you Rachel Keeffe for skinning the snakes in addition to your work. It was the Gaboon Viper Skin that you showed me which inspired this project in the first place. Thank you Heather Hamilton for teaching me how to use the electron microscope and helping me every time the machine exploded. Thank you Martha Hoopes, Alanna Hoyer-Leitzel, and Renae Brodie for being on my committee team and providing helpful critique. Thank you Rachel Fink for being my biology major advisor. Thank you to the NSF for funding Patricia Brennan's research, and therefore funding mine. Thank you to my fellow thesis students, we finally made it through. Thank you to all the lab members that helped with snakeskin tanning. I would not have time to finish this project without you, and we now have a huge collection of snakeskins for future study and display.

DEDICATIONS

Thank you apple sauce for tasting so sweet,

Thank you snakes who move without feet.

Thank you cats and your comforting purrs,

Thank you Alfredo full up on worms.

Thank you old SEM for lasting this long,

Thank you rowing for making me strong.

Thank you Jorge, may your reign last forever,

Thank you friends and family, always together.

TABLE OF CONTENTS

LIST OF FIGURES

LIST OF TABLES

ABSTRACT

The surface layer of snake scales produces patterns and textures called microstructures visible only at high magnifications. They are highly variable and responsible for snakeskin's hydrophobicity, structural color, and frictional properties. Past research has used snake shed or wet preserved skins to study these microstructures as opposed to tanned skins. Additionally, little research has been done on the microstructures formed by keratinocytes found between the snake scales and in the hinge region. We used SEM to image the anterior, middle, and posterior dorsal snakeskin microstructures of eight different snake species. We compared the scale microstructures to currently published microstructure research SEM photos and between body regions. We compared inter-scale keratinocytes between species and body regions. We found similar scale microstructures on our tanned skins to other published research. There was some variation between scale microstructure and body region. Inter-scale keratinocytes were very round for all species but varied in size across species. There was no variation in size or circularity between body regions. Tanned skin is useful for SEM research. There is more regional variation of scale microstructures than previously described. Keratinocyte characterization and how its diversity relates to microstructure would be an interest area for further research.

INTRODUCTION

Overview on Snake Integument

Snakes are found in the majority of the planet's biomes, only limited by cold temperatures (Mattison 2008). They can climb, swim, and dig in addition to slithering on the ground (Mattison 2008). Snakes can traverse a diverse array of environments, despite not having legs. Instead, the snake's skin is responsible for movement.

Skin has a complex job. Skin provides a barrier between the organism and its environment. This barrier is especially important for amniotes (mammals, reptiles, birds), as it allows them to live on land and reproduce away from water. Reinforced barriers are needed to protect against desiccation (water loss) as they are no longer constantly surrounded by water (Alibardi 2003). Living on land also creates points of high contact pressure where the animal meets the ground, which also calls for reinforcement. However, with increased toughness comes less flexibility. Reasonably, for the animal to move, the skin needs to move as well. For organisms to live on land full time, they need to solve the problem of balancing protection and movement.

The reptile's answer to this conundrum is keratinized scales. The skin is folded in on itself to create scales (or scutes) (Maderson 1964). The scales are then reinforced to provide protection and the skin in between the scales is left soft to allow the scales to move. This makes the reptile's skin both tough and able to

move and flex (Maderson 1964). The shape, size, and color of scales are extremely variable and specific to reptile species. The arrangement of scales is often used for accurate species identification (Rutland et al. 2019). The scales also often correlate with the animal's ecology and habitat (Mattison 2008). Scales have often become highly specialized for use besides protection. Scales can be colored to provide camouflage, and some species can change their colors on the fly to communicate (Rutland et al. 2019). In rattlesnakes, the scales of the tail have been adapted to vibrate against each other when shaken, creating a clear warning sound to potential predators (Rutland et al. 2019). Geckos have specialized scales lining their toes that allow them to climb completely smooth surfaces (Rutland et al. 2019). What was simply a way to protect the animal from the harsh environment on land has transformed into a variety of useful adaptations.

Scales existed in fish before the appearance of reptiles. However, the structure of reptile scales is quite a bit different from fish scales. Unlike fish scales, the scales of a reptile are reinforced with stiff beta-keratin (Rutland et al. 2019). The skin's mechanical plasticity is retained by having the skin between the scales be made of mainly alpha-keratin, which is flexible and present in all vertebrates (Rutland et al. 2019). The differentiated layers of the epidermis allow for these different flexibilities (Maderson 1964). The outermost layer of the skin is the oberhautchen layer, which is a thin layer of skin made up of cells called oberhautchen cells (Rutland et al. 2019). Below this is the beta layer, in which a thick layer of beta-keratin is found. The third layer down is the mesos layer,

which contains mostly lipids (Rutland et al. 2019). The layer below that is the alpha layer, which contains mostly alpha-keratin (Rutland et al. 2019). The bottom most layer is the stratum germinativum, which contains keratinocytes (Figure 1) (Rutland et al. 2019). When it comes to snakes, their scales overlap each other and are only attached to the skin on their cranial end. The attachment point is called the hinge region and is where the reinforced scale transitions into the more flexible inter-scale skin (Maderson 1964).

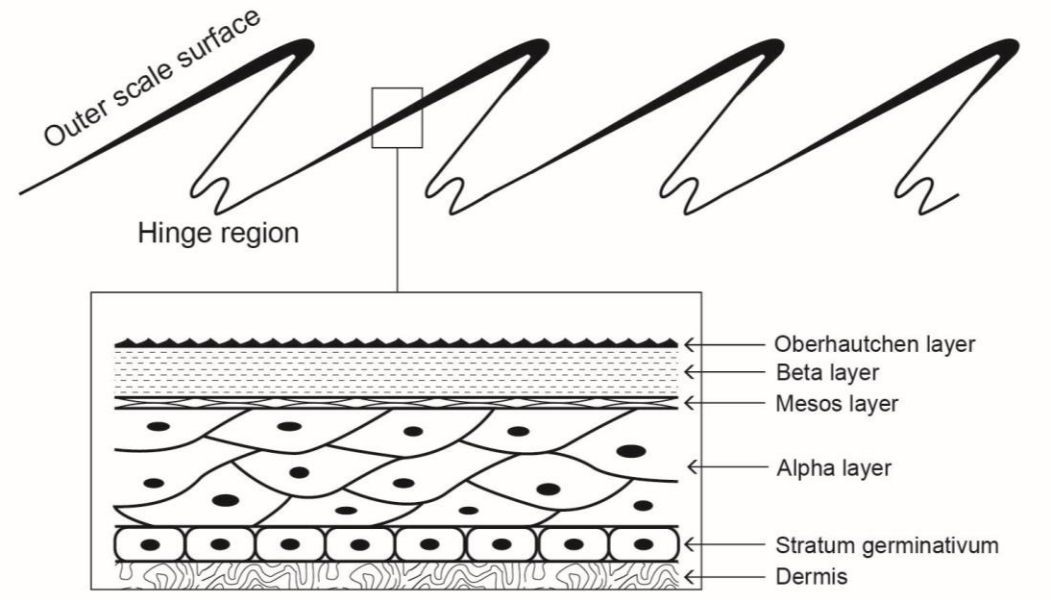

Figure 1. Diagram illustrating the layers of snakeskin in transverse section. Modified from Sacha et al. 2020 and Schmidt and Gorb 2012

Snakeskin Microstructure

The surface of reptile skin is full of microscopic textures produced largely by the oberhautchen cells. The microstructure is also affected by the layers underneath the oberhautchen layer (Harvey 1993). These textures have been described many times, often under different names including microornamentation (Picado 1931), microdermatoglyphics (Price 1982), nanostructure (Arrigo et al. 2019), and ultrastructure (Chiasson and Lowe 1989). For this study, we will be referring to these textures as microstructures. They were first described by Leydig (1868), who also observed that they might be useful for taxonomic purposes (1873). Leydig and others who studied microstructures at the time would only have access to light microscopy, which only allows very large features of the microstructure to be seen, such as the outlines of the oberhautchen cells.

Seeing the true complexity of these microstructures requires electron microscopy. Electrons have a much smaller wavelength than light on the visible spectrum, so they are used to attain images at much higher resolutions. Using Transmission Electron Microscopes (TEM), many studies verified the taxonomic value of microstructures (Hoge and Santos 1953). Scanning Electron Microscopes (SEM) are especially useful for this type of research, as they produce an image of the surface features present on a sample. Studies that have used this type of imaging have found that types of microstructures correlate strongly with phylogeny (Arrigo et al. 2019).

Although microstructures are mostly influenced by phylogeny, phylogeny alone does not explain the full variation we see in these microstructures. Microstructures have been found to have functional characteristics, and therefore could be influenced by the snake's habitat (Schmidt and Gorb 2012).. For example, microstructures create the structural colors seen on snakes like the Gaboon viper (*Bitis rhinoceros*). Their microstructure enhances the dark regions of their skin, making them appear velvety black, and this coloration allows them to better camouflage in their environment (Spinner 2013). Some fossorial snakes such as the sunbeam snake (*Xenopeltis unicolor*) have an iridescent sheen to their scales, caused by evenly spaced ridges in their microstructures (Dhillon 2014). This is likely a by-product of being a fossorial species, as these microstructures also prevent the skin from being contaminated by dirt and water (Gans and Baic 1977). On the ventral scales, the microstructures have been shown to cause frictional anisotropy, resulting in low friction when moving forward and higher friction during backwards movement. This prevents backwards movement when the snake is moving, which helps the snake move in the absence of legs (Hazel et al. 1999). These microstructures help the snakes live in their environments, so variation here is influenced by ecology as well and not only phylogeny.

There are other influences on microstructure as well. When snakes are first born, they have microstructures that are different from the adults of the same species. Their microstructure only resembles the adult's after their first shed (Price 1989). The microstructures visible before and after shedding are also

slightly different at all ages due to typical wear and tear (Cole and Van Devender 1976). Microstructures are also variable depending on their location on the scale (Gower 2003). Some scales are smooth, while other scales have a ridge going down the middle called a keel. The microstructures found on the ridge of a keeled scale are different from the rest of the scale (Chiassion 1981). Some scales also have apical stigmata, which are small divots in the scale surface, and the microstructures found inside the divot are different from the ones found on the rest of the scale (Chiassion and Lowe 1989). The ventral and dorsal scales can also differ in microstructures, as the ventral scales are more often in contact with the substrate than the dorsal scales (Arnold 2002). However, in some fossorial snakes, the microstructures found on the circumference of the midbody had no differences, as these snakes are fully surrounded by their substrate (Gower 2003).

Motivation and Goals of this Study

The nature of Dr. Brennan's research provides the lab with a large variety of snakes. Although only the posterior region is needed for the genital morphology study, our lab usually acquires whole snakes, and we have begun removing whole skins of several species to create a snakeskin collection. The diversity we have seen in snakeskin patterns and scales prompted my interest to pursue this thesis work. Here we will examine three questions: 1) Are the microstructures found in tanned skin comparable to those found in shed skin and

wet preserved skin? 2) Are the microstructures found in the anterior, middle and posterior parts of the dorsal skin of the snake comparable, or are there regional differences? and 3) Are the keratinocytes of the alpha layer similar or different across species and body regions?

To preserve these snake skins, we have been using a tanning solution and having the skins dry completely, as opposed to preserving them in formalin or alcohol. For microstructure studies, this type of sample preparation is not typical as the few currently published studies that use whole skin use fluid preserved samples. The vast majority of SEM snake microstructure imaging uses the shed skin as opposed to whole skin. Lepidosaurs regularly shed their outer epidermis, in which they reveal a fully formed new epidermis underneath, and this old skin contains all the layers of skin mentioned previously (Oberhautchen layer to alpha layer). It is reasonable to expect that the shed skin and the full skin would show similar microstructures. The surface of the shed contains the oberhautchen layer and all the microstructures it produces with it. However, shed skin is worn skin. The microstructures on the oberhautchen layer can be damaged and contaminated, and the shed skin is the oldest and most damaged by nature (Cole and Van Devender 1976). The underside of the shed is made up of a layer called the clear layer and contains a mold of the surface of the new oberhautchen layer (Irish et al. 1988). The clear layer would then contain a mold of the new and undamaged microstructures, but they also contain the outlines of the cells that make up the clear layer. These outlines of the clear layer cells and the outlines of the

oberhautchen cells can be hard to differentiate (Irish et al. 1988). Snake sheds are fragile and can be broken or eaten by detritivores if not stored correctly. Snake sheds are also not always available, as in our case, where our received specimens were already deceased.

In the existing studies where the actual skin was used, the samples were preserved in fluid, using ethanol or formalin first, which is typical for organic samples. However, since SEM imaging is done under a high vacuum, wet samples would be damaged in that environment. Although there are processes available to dehydrate organic samples, the technique is time-consuming and can involve hazardous chemicals. The advantage of using the tanning process is that the final product is a completely dry specimen that can be used directly in the SEM. Shed skin is also completely dry, but for the reasons previously stated, we could not use them in our study. One goal of this study is to determine if the microstructures on tanned snakeskin samples are comparable to wet preserved samples and shed skin samples.

When looking at the regional differences in microstructure, most previous studies have compared dorsal versus ventral scales. Differences in the microstructure of ventral and dorsal scales were noticed very early on using light microscopy (Pockrandt 1937), which were also verified by SEM imaging (Schmidt and Gorb 2012). Picado (1931) also concluded with light microscopy that microstructure is consistent in different body regions of the snake. However, Gans and Baic (1977) found that microstructures on the tails of uropeltid snakes

had spines and ridges, while the rest of the body was smooth. The body scales would prevent the adhesion of soil particles while the tail would encourage it, creating a dirt plug at the end of the tail that the snake then uses to close up the end of its burrow. This is the only study available that compares the microstructures of different body regions. There are other examples of snakes having different types of scales on different body regions, like the keeled tail scales of male *Liodytes alleni* (Jackrel 2012). The SEM photos of snake microstructures by Allam and Abo-Eleneen (2012) show differences between the head, trunk, and tail scales. We want to determine if there are differences in snake microstructures between the anterior, middle, and posterior regions of the trunk dorsal scales.

While learning how to use the SEM, we came across microstructures that we were not expecting. On the hinge region of the snakeskin, we observed round structures that were highly visible at x1000 magnification, compared to the x3000 and x9000 needed to see most of the on-scale microstructures. It is likely that these microstructures are formed by keratinocytes, specifically the fully keratinized cells of the alpha layer. Keratinocytes are cells that produce keratin. Undifferentiated keratinocytes are in the stratum germinativum. As they multiply they get pushed to the surface of the skin. As the cells get pushed out they differentiate into the upper layers of the epidermis, eventually becoming fully keratinized and dying. In the order Squamata, the cells in the beta layer are syncytial, meaning they are no longer separate cells and have coalesced into a

compact layer (Horstmann 1964). In the alpha layer, the keratinocytes are still distinct from each other. On the surface of the scales, the beta layer is thick. In the hinge region, the beta layer is much thinner, and the shapes of the separate alpha layer keratinocytes can be seen (Alexander 1970). SEM images of keratinocytes also look like the structures we found (Mobasseri et al. 2019). We want to characterize these keratinocyte structures to determine if they differ between species and between anterior, middle, and posterior body regions on the trunk, since they do not seem to have been studied before.

In this study, I used tanned snake skins to observe, quantify, and compare the dorsal microstructures of 8 snake species. Out of our available snakeskins, we chose eight snakeskins that covered a large spectrum of species, taxa, and ecology to see as much diversity as possible. We took samples from the anterior, middle, and posterior regions of the dorsal trunk of the snake. Using SEM, we photographed the dorsal microstructures on the scales and between the scales. We compared the scale microstructures found on the tanned samples to the microstructures reported in other studies. We qualitatively compared the scale microstructures between the body regions sampled on the snake. We also quantified the images of the inter-scale keratinocytes and compared them between species and body regions.

MATERIALS AND METHODS

Study Species

The dorsal scales of eight snakeskins from different species were examined. Species were chosen to represent a large ecological diversity from specimens in our collection. Our selected snakeskins contained two arboreal, two terrestrial, two aquatic, and two fossorial species. We also have large phylogenetic diversity in our selection with four Colubrids, two Pythons, one Psammophiid, and one Xenopeltid. Only one member of each species was studied.

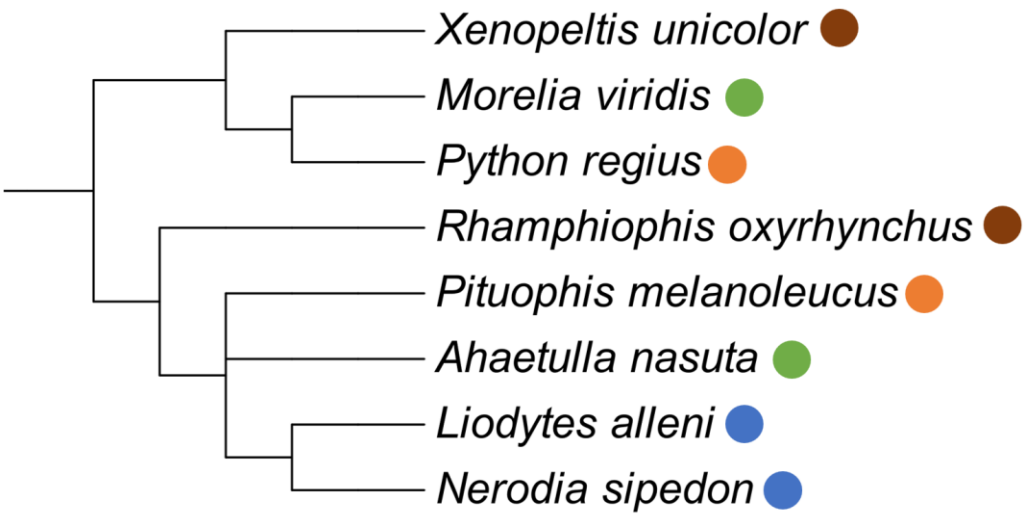

Figure 2. Phylogeny of examined species. The ecology of snakes is marked as such: Arboreal (green dot), Terrestrial (orange dot), Aquatic (blue dot), and Fossorial (brown dot). Assembled using PhyloT using the database created by Schoch et al. 2020.

Ahaetulla nasuta, or the long-nosed whip snake, is a colubrid native to the rainforests of Sri Lanka (Wall 1921). It is bright green and slender and has a distinctive long and pointed face (Wall 1921). The snake can enlarge its body when threatened, causing its scales to separate, and revealing a striped black and white pattern underneath (Wall 1921). Its dorsal scales are smooth.

Morelia viridis, or the green tree python, is a python native to the rainforests of Indonesia, Papua New Guinea, and Australia (Hillman 2010). The adults are bright green, but juveniles are corn yellow or brownish red, and eventually grow into its green color (Hillman 2010). Many adult green tree pythons have an unbroken line or a line of spots of white/yellow scales on their back going down the length of the snake (Hillman 2010). Its dorsal scales are smooth.

Pituophis melanoleucus, or the eastern pine snake, is a colubrid native to the eastern United States, and lives in a variety of environments (Rasmussen 2012). It can be found in pine and oak forests, high and dry rocky ridges, sand hills and fields (Rasmussen 2012). It is a large snake with dark brown and black splotches on its back, and a cream white underbelly (Rasmussen 2012). Its dorsal scales are keeled.

Python regius, or the ball python, is a python native to savannah grasslands and open forests of West and Central Africa (Graf 2011). The typical ball python has white ventral scales and light to dark brown splotches on its back

(Graf 2011). It is popular in the pet trade due to its slow movement and easy handleability (Graf 2011). Its dorsal scales are smooth.

Nerodia sipedon, or the northern water snake, is a colubrid native to the northeastern United States (Gillilland 2013). It lives in many different freshwater environments like lakes, rivers, and wetlands (Gillilland 2013). It can move on land but it does not often venture far from its aquatic environment (Gillilland 2013). It is a dark gray snake with orangish brown alternating splotches or bands (Gillilland 2013). Its dorsal scales are keeled and have two large apical stigmatas, one on each side of the keel (Chiassion and Lowe 1989).

Liodytes alleni, or the striped crayfish snake, is a colubrid native to Florida in the United States (Jackrel 2012). It is found in freshwater environments that are often full of floating vegetation like water hyacinth (Jackrel 2012). The high-density vegetation attracts crayfish, the snake's prey, and provides shelter from predators (Jackrel 2012). It is a dark olive-brown snake with three yellow brown stripes that extend lengthwise down its back (Jackrel 2012). Its dorsal scales are smooth except for some keeled scales on the tail in males (Jackrel 2012). Our studied specimen is female, so we did not see the keeled scales.

Rhamphiophis oxyrhynchus, or the Rufous Beaked Snake, belongs to the family Psammophiidae and is native to east Africa (Branch 1998). It lives in bushland environments, and it shelters in the burrows of small mammals and

termites (Branch 1998). It is a reddish-brown snake with a creamy underbelly (Branch 1998). Its dorsal scales are smooth.

Xenopeltis unicolor, or the sunbeam snake, belongs to the family Xenopeltidae and is native to southeast Asia (Das 2015). It typically lives in old-growth forests, and it spends much of its time hidden underground in rodent burrows and leaf litter (Das 2015). It is known for its dorsal iridescent scales and is overall a brown color with a white underbelly (Das 2015). Previous studies have shown that the microstructures present on its dorsal scales are at least partially responsible for their iridescence (Dhillon 2014). Its dorsal scales are smooth.

Specimens

Deceased snakes were collected from snake breeders, zoos, and other scientists. Some snakes were purchased using an NSF Career award to P. Brennan IOS- 2042260. The snout to vent length (SVL) of the snakes were measured for whole, intact specimens. Some snakes had their head removed before we received them but were intact otherwise. If the snake was headless, we measured from the vent to the distal anterior end of the snake for the SVL.

Tanning

Skins were cut down the midsagittal plane on the ventral side of the snake, where it was peeled and removed from the rest of the body. The remaining flesh attached to the skin was removed using tweezers, dull scalpels, and scissors until only the clean skin remained. The skin was then laid flat, scale side down, on a long wooden board. Using a foam brush, a thin layer of Deer Hunter's & Trapper's Hide Tanning Formula™ was applied and spread evenly. Small wooden blocks and metal weights were placed on the edges of the skin to prevent the skin from curling while drying. After 24 hours of drying, another thin coat of tanning formula was applied. Further coats were added after drying if the skin was still brittle, waiting 24 hours between new coats. Preserved skins were then labeled and stored between paper and cardboard layers to keep them dry and flat. Small clippings of the tanned skins were taken and stored between labeled paper and cardboard to be prepared for SEM. Regional samples were collected from the anterior, middle and posterior trunk regions of each snake as shown in Figure 3.

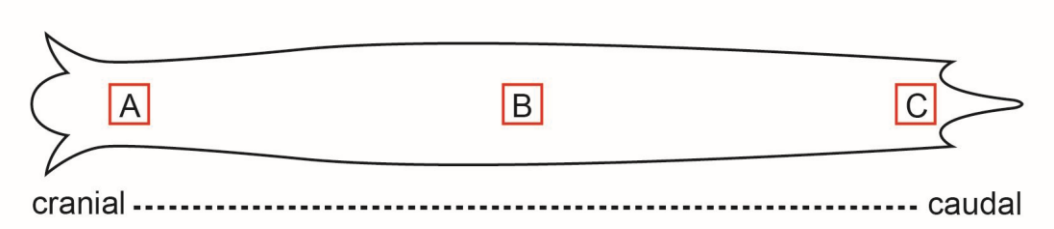

Figure 3. Locations of (A) anterior, (B) middle, and (C) posterior dorsal trunk region samples. Anterior samples were taken immediately posterior to the back of the head. Posterior samples were taken immediately anterior to the cloaca. Middle samples were taken at the halfway point between the anterior and posterior samples.

Scanning Electron Microscopy

Skin clippings were put in the vacuum oven at room temperature for 24 hours. Clippings were then trimmed to the area of interest then attached to SEM stubs using carbon tape and sputter coated with gold. All SEM imaging was performed on the FEI Quanta 200™ using the secondary electron detector. Photos detailing the overall scale morphology and orientation were taken at x35 magnification. Photos of the microstructures on the dorsal scales were taken at x1000, x3000, and x9000 magnification at the caudal tip of the scale (Figure 4, location B). Images of the inter-scale keratinocytes were taken at x1000 magnification if visible (Figure 4, location A).

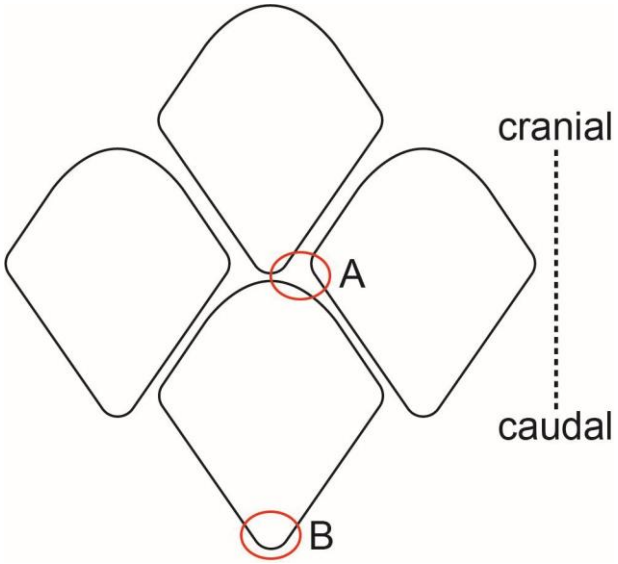

Figure 4. Schematic figure of the examined positions on the dorsal snakeskin, marked by red circles. (A) Image location of the inter-scale keratinocytes. (B) Image location of the scale microstructures.

Measurements

All measurements and image edits for the microstructures and keratinocytes were made in Fiji (Schindelin 2012). The scale is set by using the set scale function and the scale bar present in the SEM images.

Scale microstructures were compared using images at x1000, x3000, and x9000 magnification. If the image had significant arching artifacts (seen as random white pixels or ‘snow’), the despeckling tool was used to remove them. The image was then contrasted using Contrast Limited Adaptive Histogram Equalization (CLAHE) using the CLAHE function in Fiji.

Inter-scale microstructures were measured at x1000 magnification. A diagonal line was drawn between the top left corner and the bottom right corner of the image. Any fully visible structures that touched the line were outlined using the polygon selection tool. Outlined structures had their area and circularity (4π*area/perimeter^2, ranges from 1.0 to 0.0, with 1.0 being a perfect circle) measured (Figure 5). The number of fully visible structures in the image were counted as well.

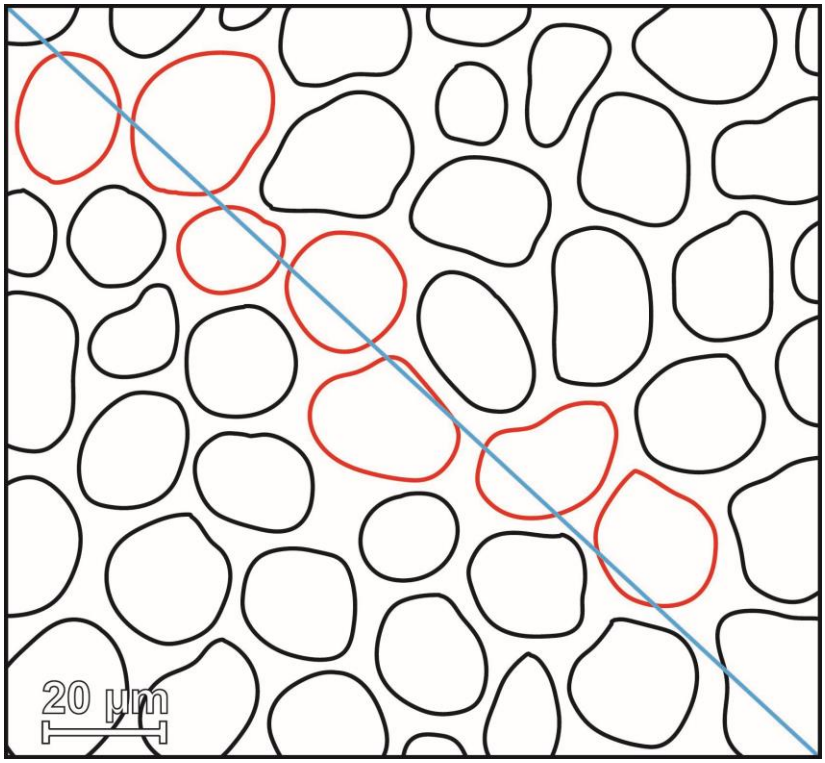

Figure 5. Schematic figure of the measured elements in the inter-scale keratinocyte images. Keratinocytes outlined in red had their area and circularity measured.

Image Analysis

Scale microstructure images were compared with existing published images taken of snake sheds. If no snake shed images were available, published images of wet preserved skin were used. Scale microstructures taken on anterior, middle, and posterior sections of the snake trunk were also compared to each other. The scale microstructures were described using methods modified from Arrigo et al. (2019). Cells borders that had many protrusions from the cell (seen as a zig-zag border or finger like extensions) were said to have denticulations. Denticulations were also described as either being regular (all being around the same size and evenly spaced) or irregular (differing sizes and spacing). Cell borders that were rounded or smooth with no protrusions were said to have no denticulations. The texture of the surface of the cells were described as having holes (small circular divots), straight channels (long straight divots that are mostly parallel to each other), labyrinthine channels (long divots that curve), or being smooth (no visible texture). Scale microstructures were said to have ridges if there were long, straight, raised areas that continued unbroken over multiple cells. These ridges are often visible at lower magnifications as they are created by multiple cells as opposed to a single cell. If ridges were not seen the microstructures were described as having no ridges.

For the inter-scale keratinocytes, the mean area and circularity of each image was calculated, along with the standard error for each mean. These values were then compared between species and body regions using a bar graph with

error bars. The mean area of all the keratinocytes for each species was also calculated and the relation between the SVL and keratinocyte size was graphed on a scatter plot.

RESULTS

Skin Preservation Method and Regional Differences

Overall, the tanned skins show very similar scale microstructure features when compared to the published data on sheds and wet specimens. The scale microstructures stayed mostly consistent between trunk body regions, but some variation was noted. Figures 6-13 compile the photos of our samples and representative photos from published works. Our original sample images without edits are available in the appendix (Figures 26-49). Descriptions of the microstructures are provided below and any differences between published photos, variation over body regions, or anomalies were noted.

Ahaetulla nasuta scale microstructures (Figure 6): The scale microstructures have ridges made up of irregular denticulations, and cell surfaces contain holes. Published shed skin image resembles the middle trunk dorsal scales most closely. The anterior scale microstructures have ridges that are barely visible, and these ridges become more distinct in the middle and posterior samples. The space between ridges appears to decrease as we move more posterior.

Morelia viridis scale microstructures (Figure 7): The scale microstructures have regular denticulations, and the cell surface is full of holes. Published shed skin image resembles the anterior trunk dorsal scales most closely. The published image has less space between cell borders than our images and describes the cell shape as being wide and elongated. Our images seem to show that the overall cell

shape is wider on the anterior trunk scales and become more rounded as we move posterior.

Pituophis melanoleucus scale microstructures (Figure 8): The scale microstructures have ridges, irregular denticulations, and the cell surface is full of straight channels. Published shed skin image resembles the posterior trunk dorsal scales most closely. The published image has more space in between ridges.

Python regius scale microstructures (Figure 9): The scale microstructures have regular denticulations, and the cell surface is full of holes. Published shed skin image resembles the middle trunk dorsal scales most closely. The quality of our skin samples or the quality of our SEM picture is poor for this specimen. The regional variance between photos is likely due to the microstructures being damaged. The denticulations can still be seen however, and the holes can be seen in the anterior image.

Nerodia sipedon scale microstructures (Figure 10): The scale microstructures have ridges, irregular denticulations, and the cell surface contains both holes and straight channels. The published paper containing the reference image was researching the apical stigmata, which we did not image. The microstructures visible in the apical stigmata are different from the rest of the scale, so our microstructure images only resembled the parts of the published images not containing the apical stigmata. The published wet preservation skin resembles the posterior trunk dorsal scales most closely. The posterior ridges are narrower than

the anterior and middle ridges. The holes and channels are not visible in the posterior image.

Liodytes alleni scale microstructures (Figure 11): The scale microstructures have no denticulations, and the cell surface is flat. The published wet preservation skin resembles the posterior trunk dorsal scales most closely. The published wet preserved image has a few sharp protrusions from the cell border. These protrusions are present in our sample but are less pronounced. We do not think these structures should be considered denticulations as they are extremely wide and only a few occur on each cell. There are also large divots present that we do not see. The cells are much more elongated in the middle and posterior images than they are in the anterior image.

Rhamphiophis oxyrhynchus scale microstructures (Figure 12): The anterior and middle scale microstructure images have been removed as we determined that the structures imaged were of damage and debris, not the scale microstructures. These removed images are available in the appendix (Figures 44 and 45). Scale microstructures have ridges, irregular denticulations and the cell surface has straight channels. The reference snake shed image is not of *Rhamphiophis oxyrhynchus* shed but instead of *Rhamphiophis rubropunctatus* shed. The paper did not provide an image of *Rhamphiophis oxyrhynchus* shed but described its microstructures as ‘caniculate’ (ridges are at close quarters forming channels between them). *Rhamphiophis rubropunctatus* shed was presented as an example of caniculate microstructures.

Xenopeltis unicolor scale microstructures (Figure 13): The scale microstructures have regular denticulations, and the cell surface is flat. The published shed skin resembles the anterior trunk dorsal scales most closely. Our posterior image had severely damaged microstructures that were barely visible. Luckily, there was a hole in the top layer of the skin and the microstructures were fully formed underneath. This is an example of how the shed skin microstructures and the snakeskin microstructures can look different (Cole and Van Devender 1976).

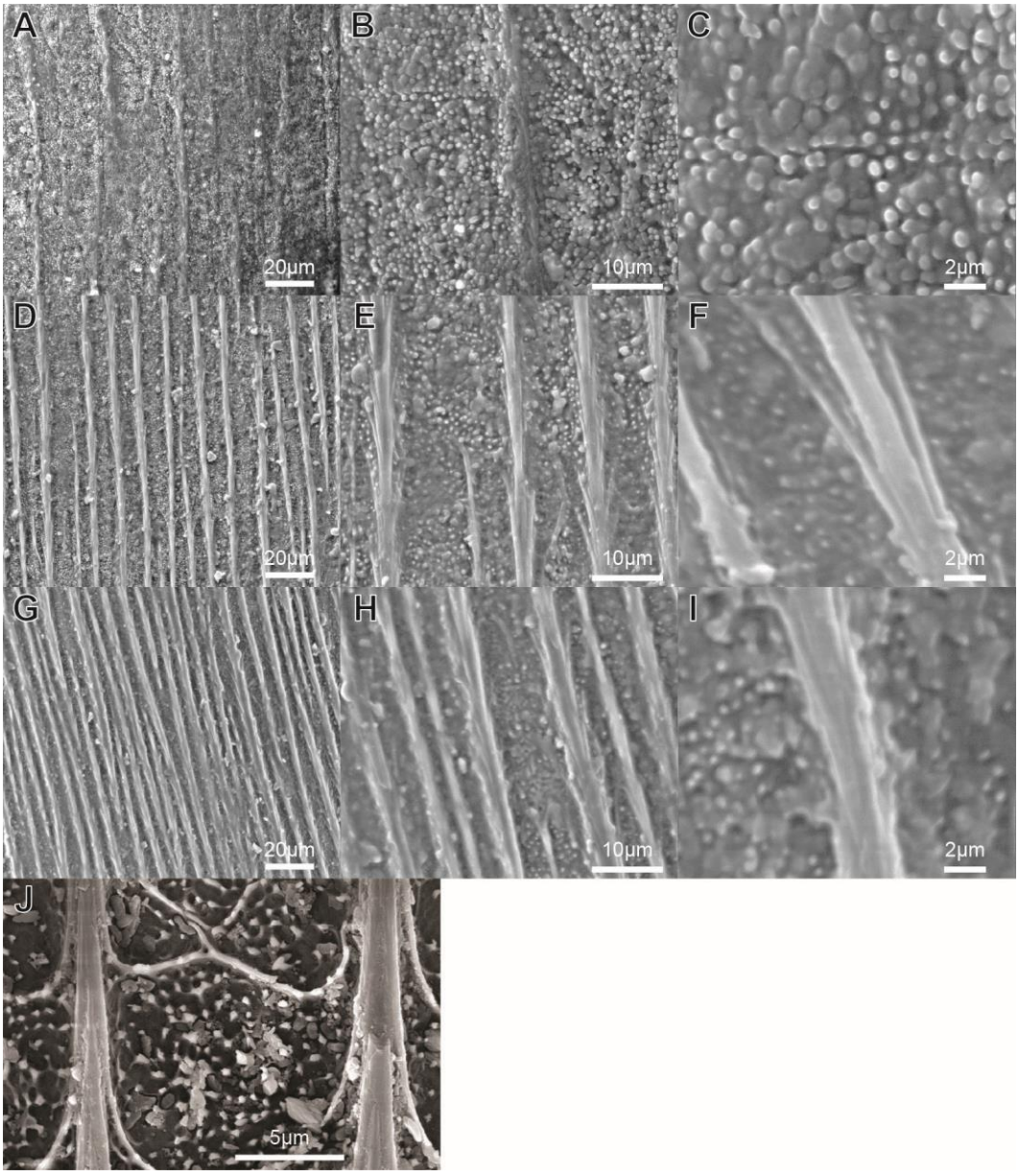

Figure 6. *Ahaetulla nasuta* (A-C) anterior, (D-F) middle, and (G-I) posterior dorsal trunk scale microstructures imaged on tanned skin. Images contrasted in Fiji. (J) *Ahaetulla nasuta* dorsal scale microstructures imaged on shed skin from Arrigo et al. 2019.

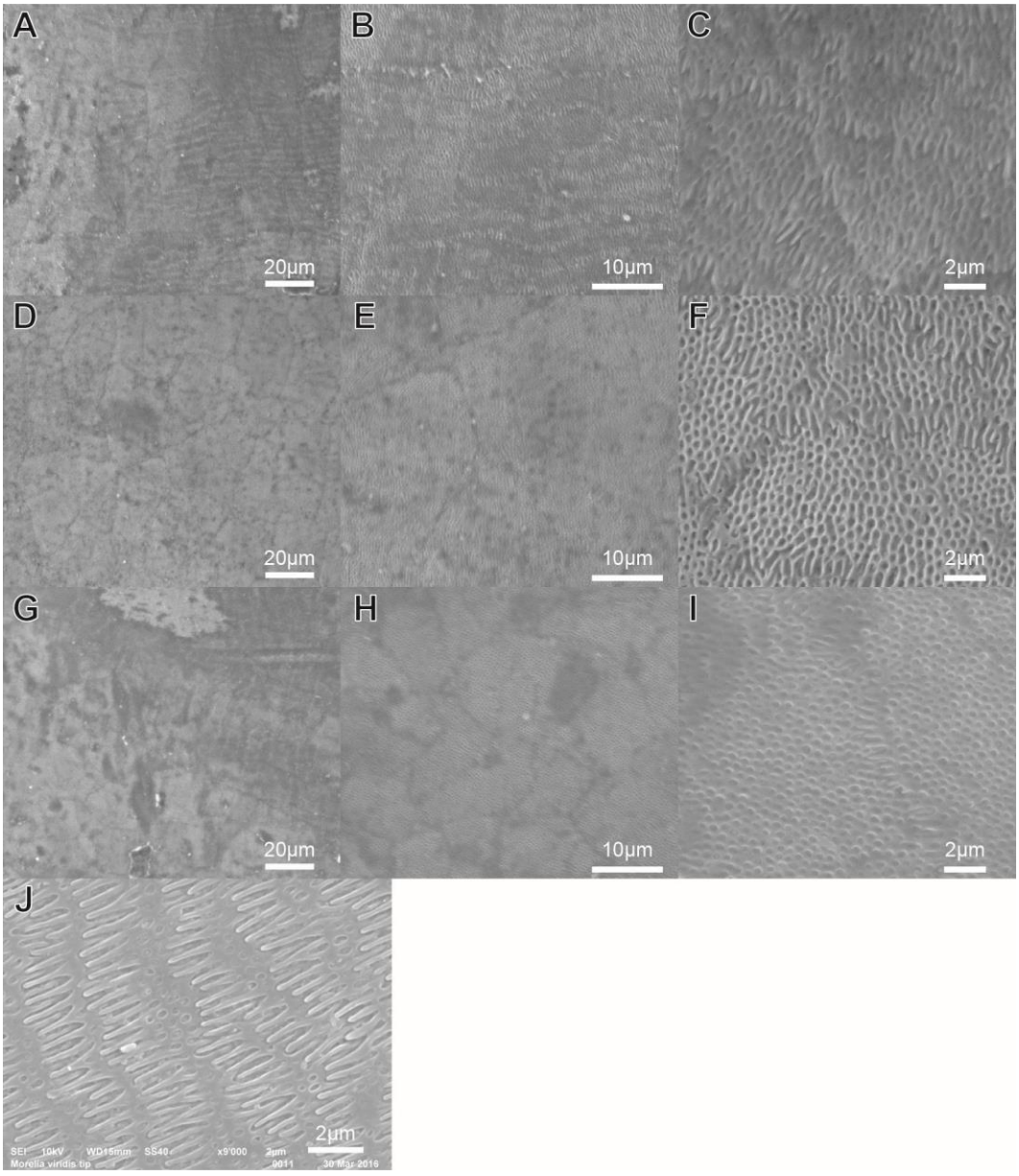

Figure 7. *Morelia viridis* (A-C) anterior, (D-F) middle, and (G-I) posterior dorsal trunk scale microstructures imaged on tanned skin. Images contrasted in Fiji. (J) *Morelia viridis* dorsal scale microstructures imaged on shed skin from Arrigo et al. 2019.

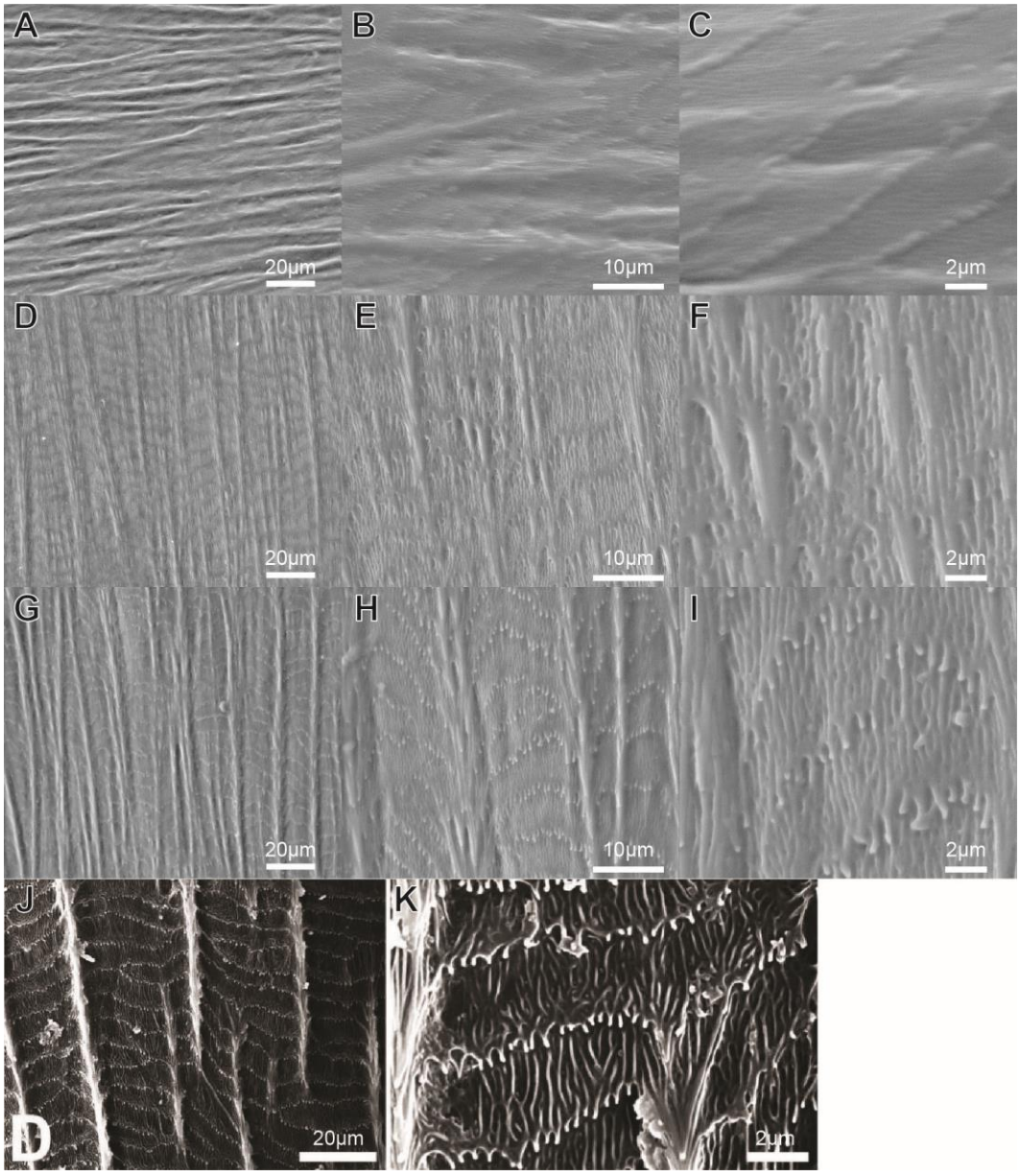

Figure 8. *Pituophis melanoleucus* (A-C) anterior, (D-F) middle, and (G-I) posterior dorsal trunk scale microstructures imaged on tanned skin. Images contrasted in Fiji. (JK) *Pituophis melanoleucus* dorsal scale microstructures imaged on shed skin from Tsai et al. 2020.

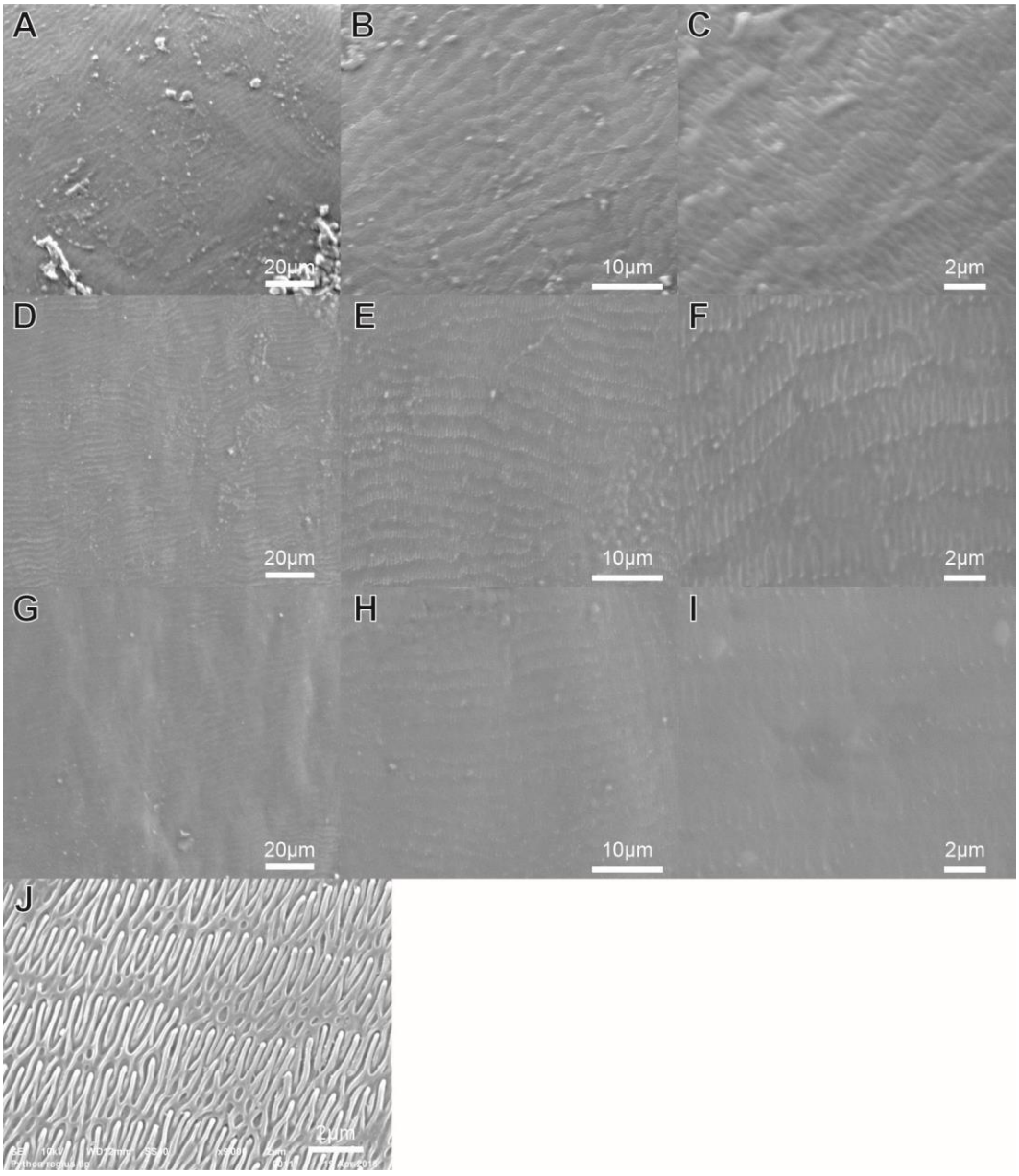

Figure 9. *Python regius* (A-C) anterior, (D-F) middle, and (G-I) posterior dorsal trunk scale microstructures imaged on tanned skin. Images contrasted in Fiji. (J) *Python regius* dorsal scale microstructures imaged on shed skin from Arrigo et al. 2019.

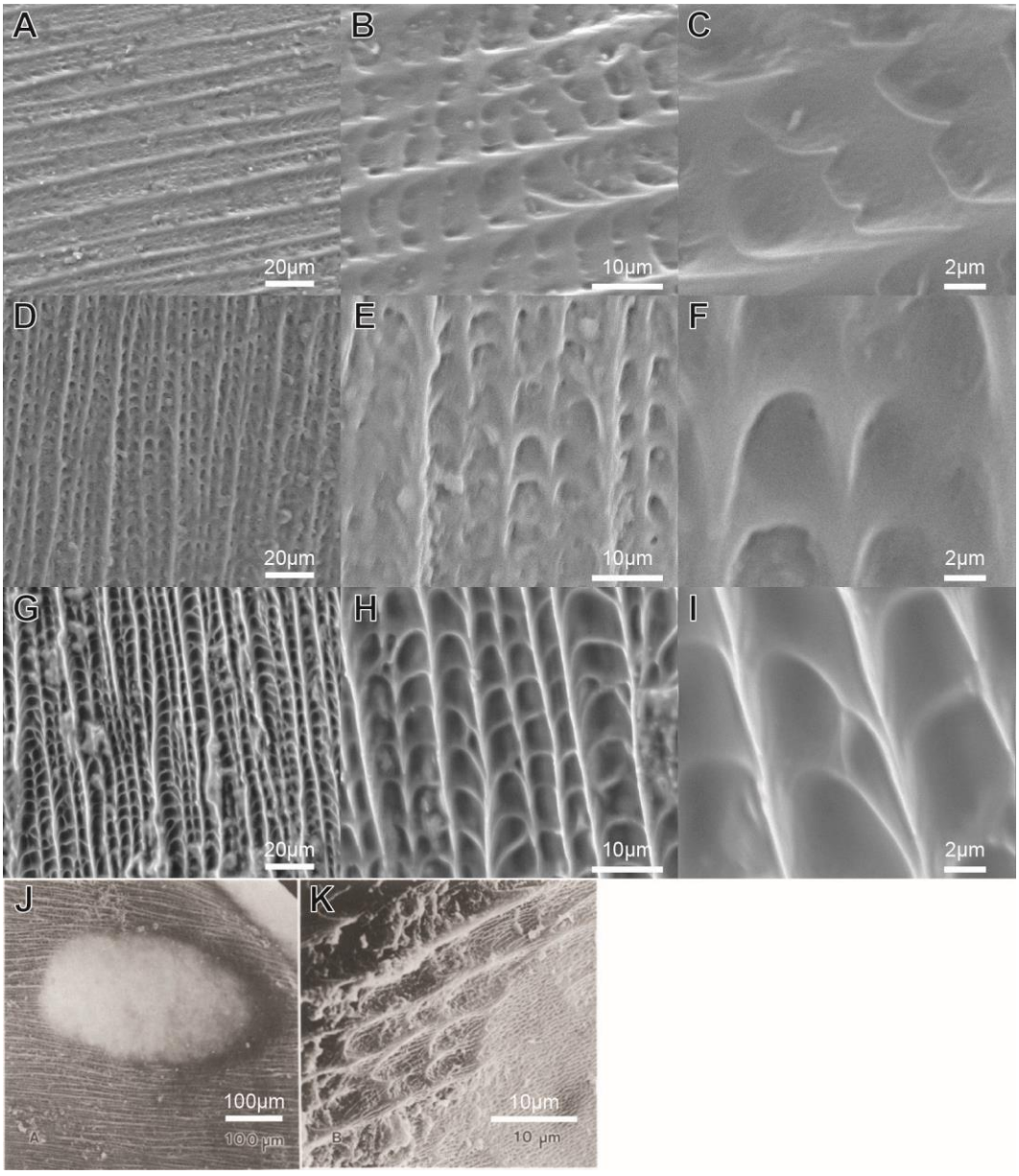

Figure 10. *Nerodia sipedon* (A-C) anterior, (D-F) middle, and (G-I) posterior dorsal trunk scale microstructures imaged on tanned skin. Images contrasted in Fiji. (JK) *Nerodia sipedon* dorsal scale microstructures imaged on wet preparation skin from Chiasson and Lowe 1989.

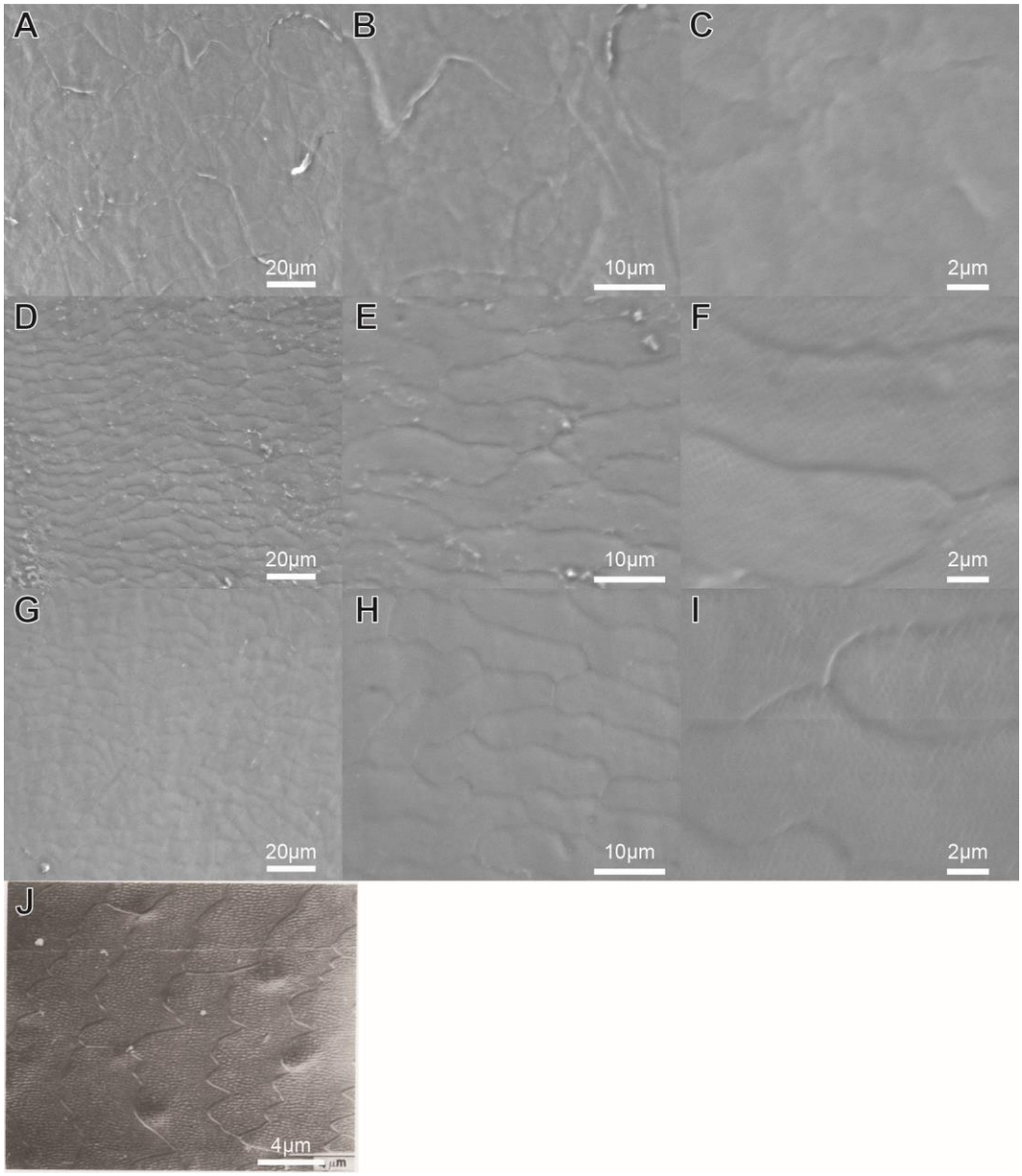

Figure 11. *Liodytes alleni* (A-C) anterior, (D-F) middle, and (G-I) posterior dorsal trunk scale microstructures imaged on tanned skin. Images contrasted in Fiji. (J) *Liodytes alleni* dorsal scale microstructures imaged on wet preparation skin from Price 1983.

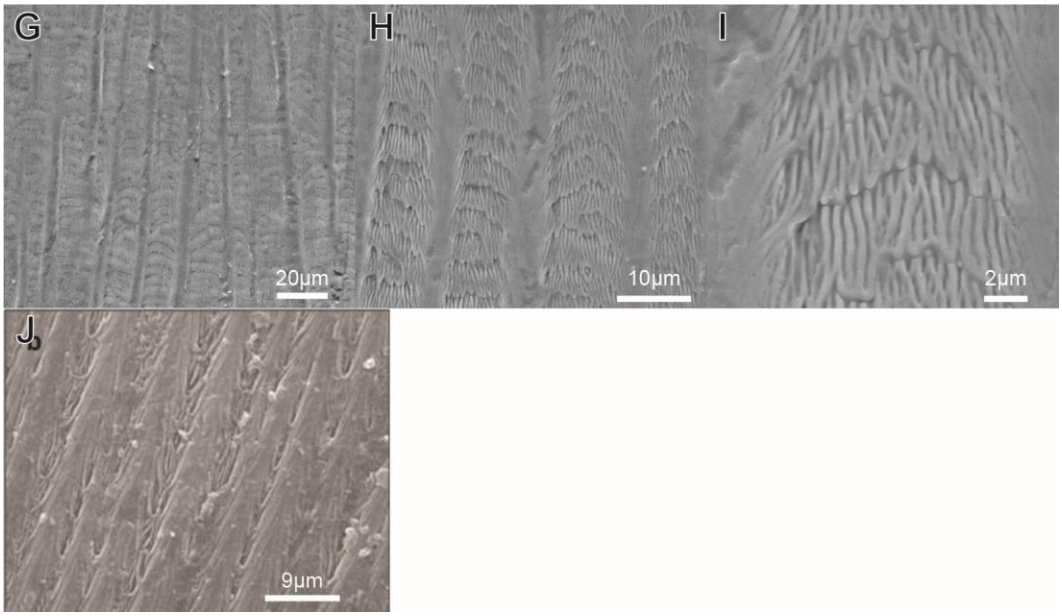

Figure 12. *Rhamphiophis oxyrhynchus* (G-I) posterior dorsal trunk scale microstructures imaged on tanned skin. Images contrasted in Fiji.
(J) *Rhamphiophis oxyrhynchus* dorsal scale microstructures imaged on shed skin from de Pury 2011.

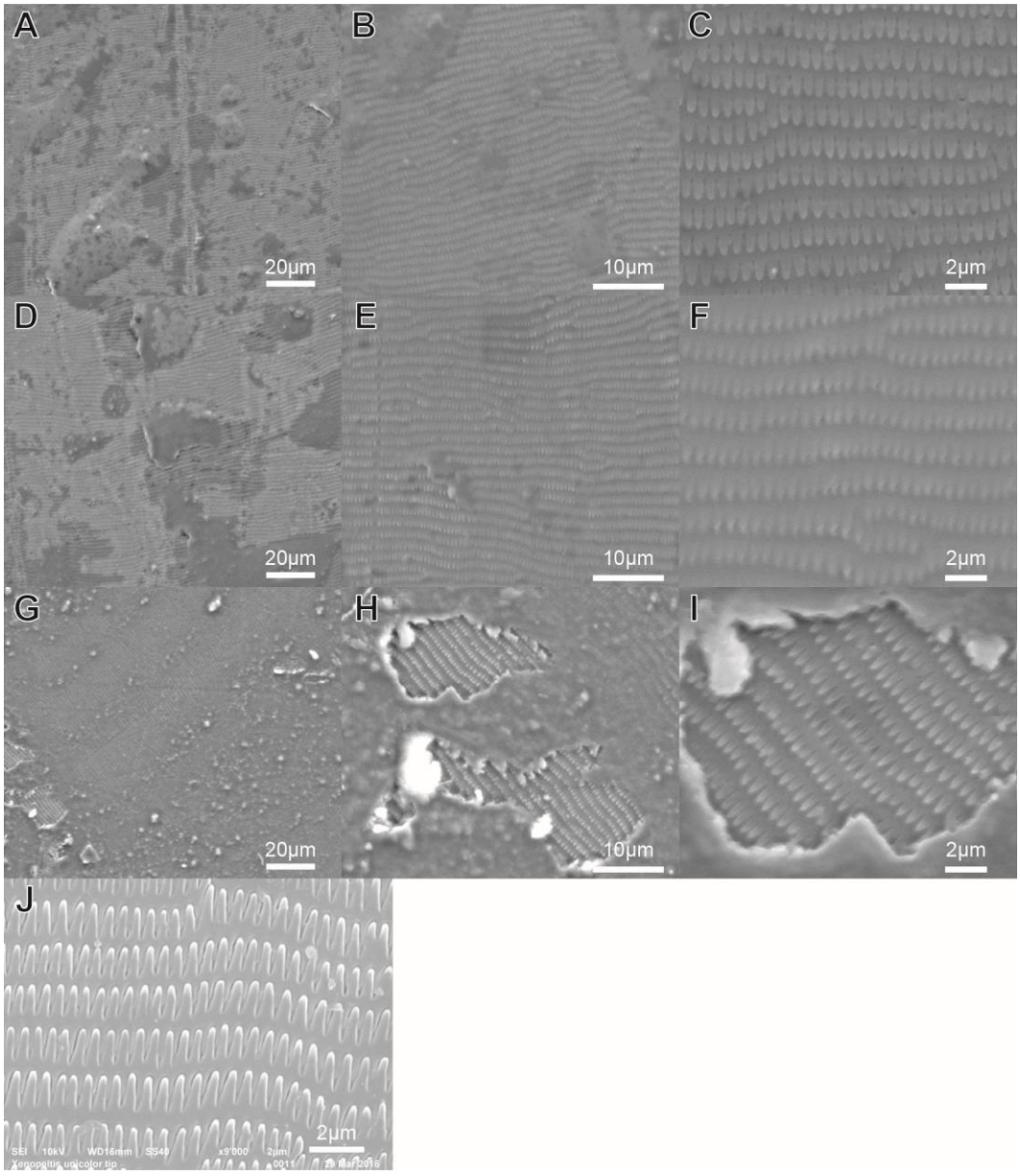

Figure 13. *Xenopeltis unicolor* (A-C) anterior, (D-F) middle, and (G-I) posterior dorsal trunk scale microstructures imaged on tanned skin. Images contrasted in Fiji. (J) *Xenopeltis unicolor* dorsal scale microstructures imaged on shed skin from Arrigo et al. 2019.

Inter-scale Keratinocyte Microstructures

We found inter-scale keratinocytes in all the specimens. All keratinocytes were rather circular between species and body regions. There were small regional differences in keratinocyte size, but there are dramatic differences in area between the species. Snakes with longer SVLs did not always have larger keratinocytes. We only had a posterior keratinocyte image for *Xenopeltis unicolor,* so we were unable to compare area and circularity mean measurements between regions. Figures 14-17 show the mean area and circularity for each photo in a bar chart along with the standard error. Figures 14 and 16 contain the same area data but are arranged differently. Figures 15 and 17 contain the same circularity data but are arranged differently. Figure 18 compares the SVL of the snake to the mean area of all the keratinocytes measured on the snake. The area and circularity measurements for the keratinocytes and the SVL for each snake specimen are available in the appendix (Tables 1-9).

Figure 14 shows that *Pituophis melanoleucus* and *Rhamphiophis oxyrhynchus* have much larger inter-scale keratinocytes than the rest of the study species. *Xenopeltis unicolor* had much smaller keratinocytes than the rest of the study species. For *Ahaetulla nasuta*, *Morelia viridis*, and *Nerodia sipedon*, the area of keratinocytes stayed mostly consistent over body regions, as the calculated standard error overlapped with each other. In *Pituophis melanoleucus*, *Python regius*, *Liodytes alleni*, and *Rhamphiophis oxyrhynchus,* the error did not account for the small difference in area mean. We are unable to test if these differences are

significant as we only had one image per body region, so our sampling is not independent.

Figure 15 shows that the keratinocytes of all species were round (circularity measurement > 0.5). Overall, the keratinocytes of *Python regius* appear to be the most elongated on average compared to the other study species. *Ahaetulla nasuta*, *Pituophis melanoleucus*, *Python regius*, *Nerodia sipedon*, and *Rhamphiophis oxyrhynchus* had variation in circularity over body regions that was not accounted for in the calculated error. Again, we are unable to test if these differences are significant as we only had one image per body region, so our sampling is not independent.

Figure 16 shows the same data as Figure 14 but is arranged to better show the variation in area between species. Figure 17 shows the same data as Figure 15 but is arranged to better show the variation in circularity between species.

Figure 18 shows that a longer SVL does not always correlate to a larger keratinocyte area. The *Pituophis melanoleucus* snake was the longest specimen and had the largest mean keratinocyte area. *Xenopeltis unicolor* had the smallest mean keratinocyte area and was the third longest specimen. *Rhamphiophis oxyrhynchus* had the second largest mean keratinocyte area but was the sixth longest specimen, only longer than the *Nerodia sipedon* and *Liodytes alleni* specimens, who both have much smaller mean keratinocyte areas. The trendline shows a positive relationship but has a low R^2 value of 0.1718.

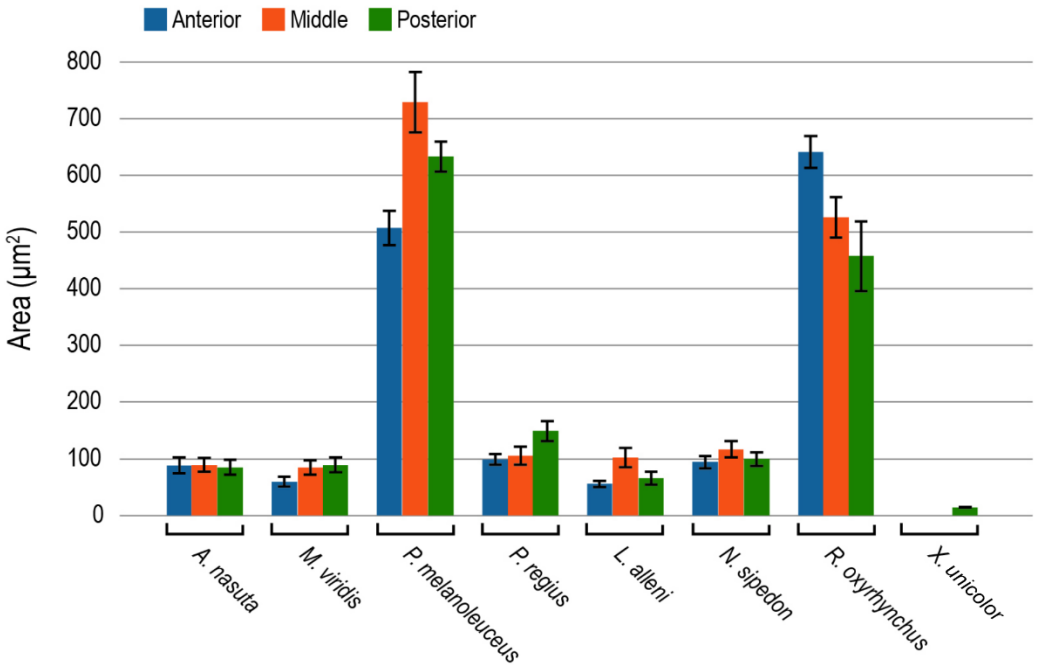

Figure 14. Bar graph of mean area of inter-scale keratinocytes, organized by species.

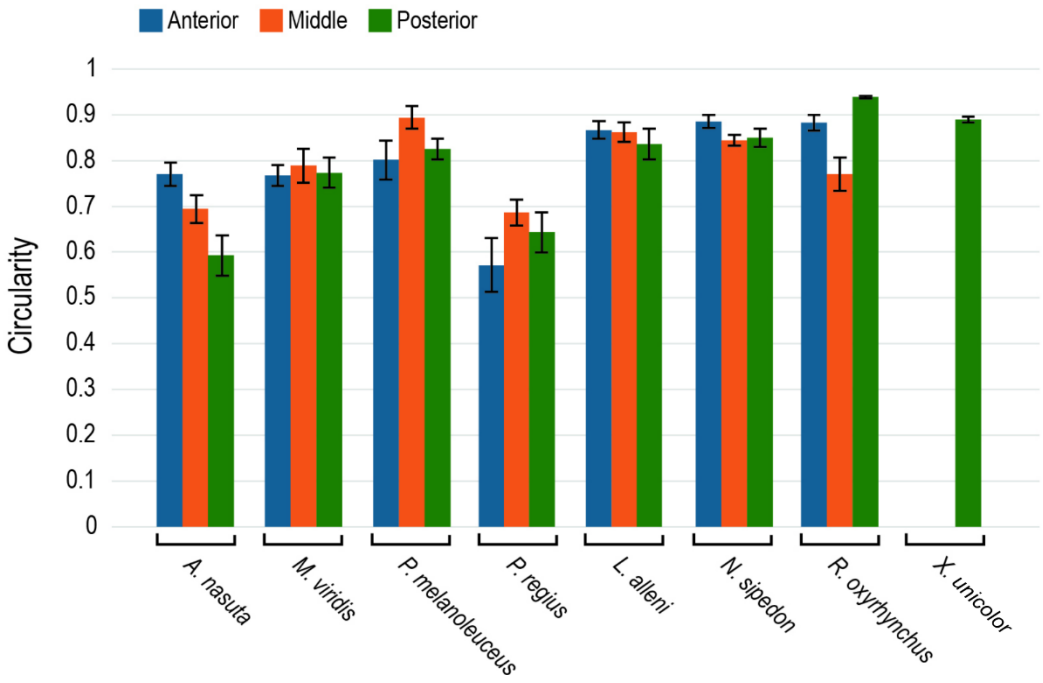

Figure 15. Bar graph of mean circularity of inter-scale keratinocytes, organized by species.

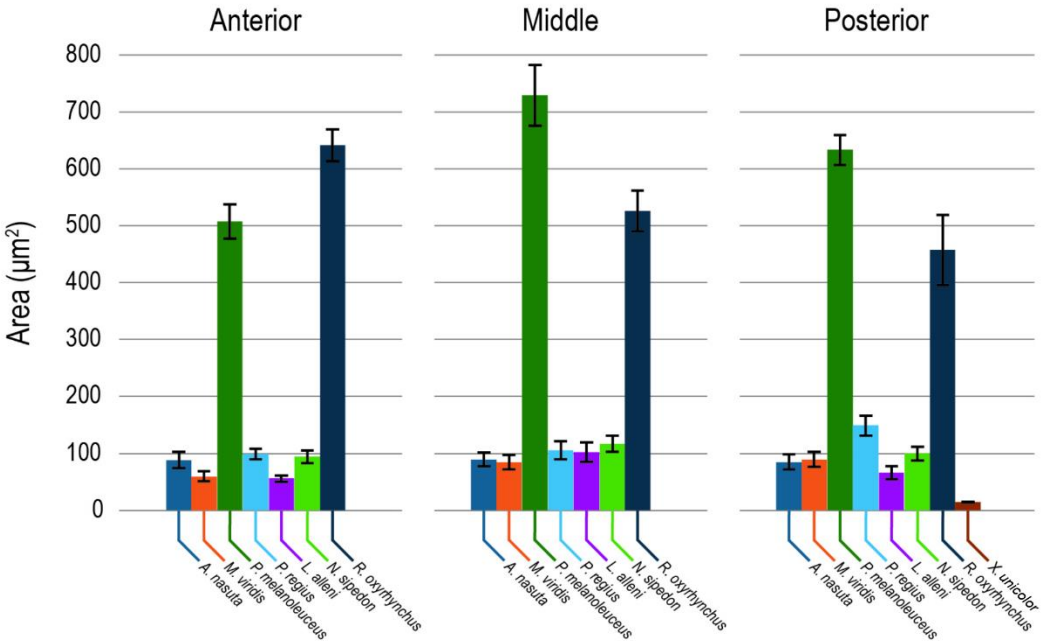

Figure 16. Bar graph of mean area of inter-scale keratinocytes, organized by body region.

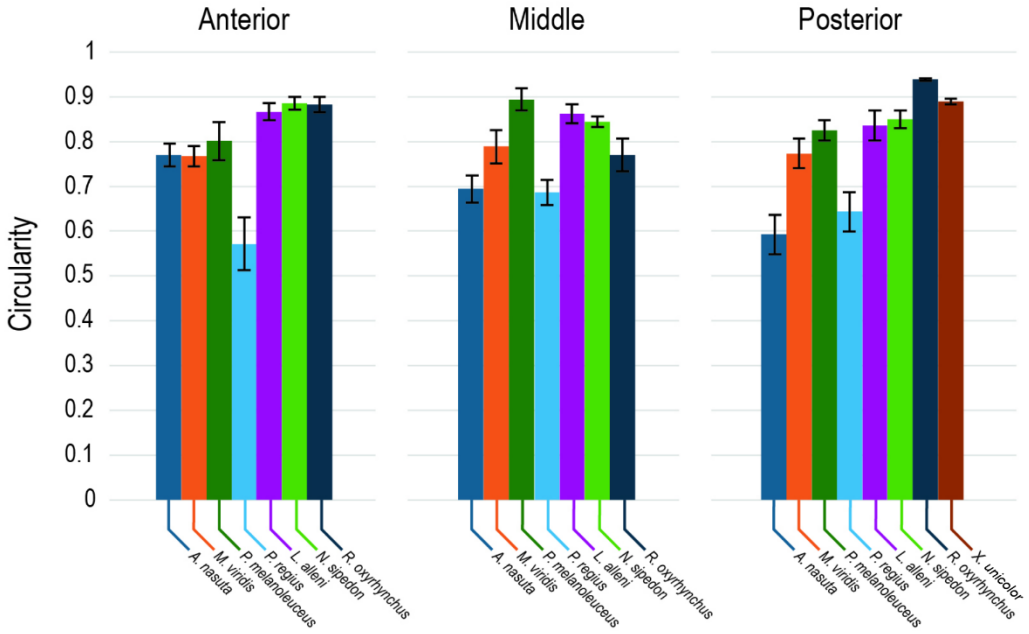

Figure 17. Bar graph of mean circularity of inter-scale keratinocytes, organized by body region.

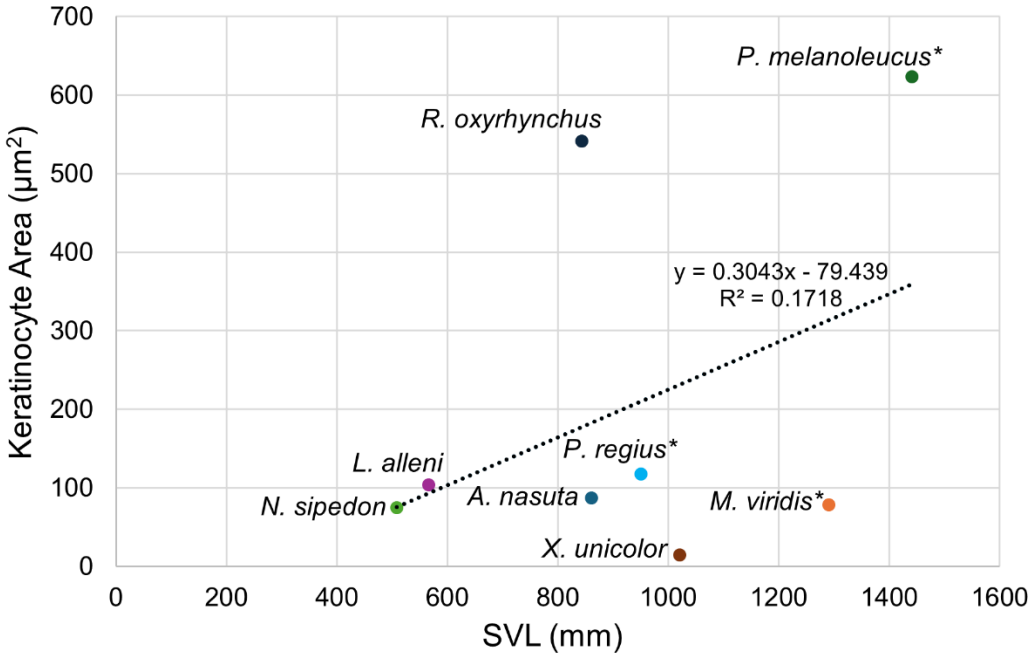

Figure 18. Scatter plot showing relationship between mean keratinocyte area and SVL for each snake specimen. *Indicates headless snake specimen, true SVL is longer than the recorded measurement

Figures 19-26 compile the photos of our inter-scale keratinocyte SEM images along with total counts of keratinocytes in the images. For *Xenopeltis unicolor* (Figure 26), only posterior inter-scale keratinocytes were visible on our specimen. The hinge region and inter-scale skin for *Xenopeltis unicolor* was completely covered and not visible in our anterior and middle skin samples. Our original sample images without edits are available in the appendix (Figures 27-50).

Counts: 110 81 103

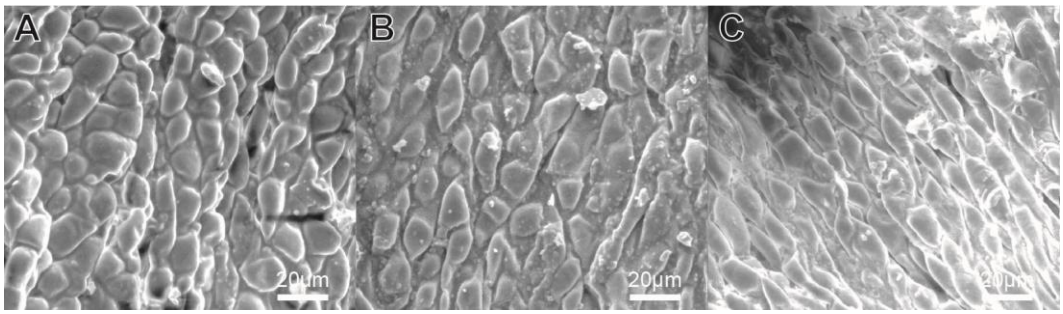

Figure 19. *Ahaetulla nasuta* (A) anterior, (B) middle, and (C) posterior inter-scale keratinocyte images at x1000 magnification.

Counts: 150 101 118

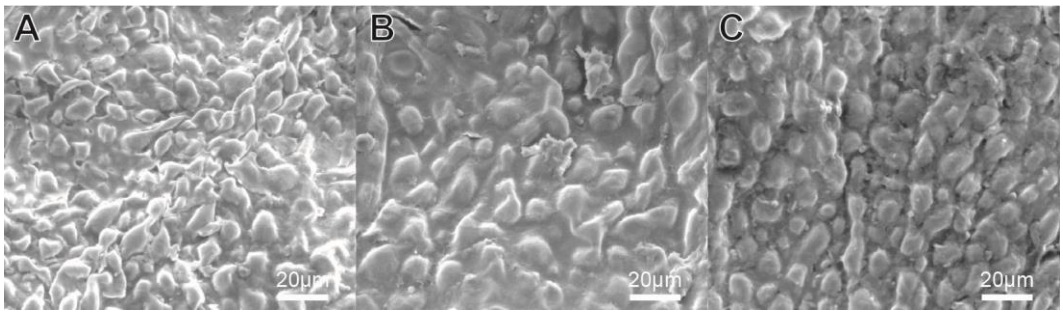

Figure 20. *Morelia viridis* (A) anterior, (B) middle, and (C) posterior inter-scale keratinocyte images at x1000 magnification.

Counts: 23 16 17

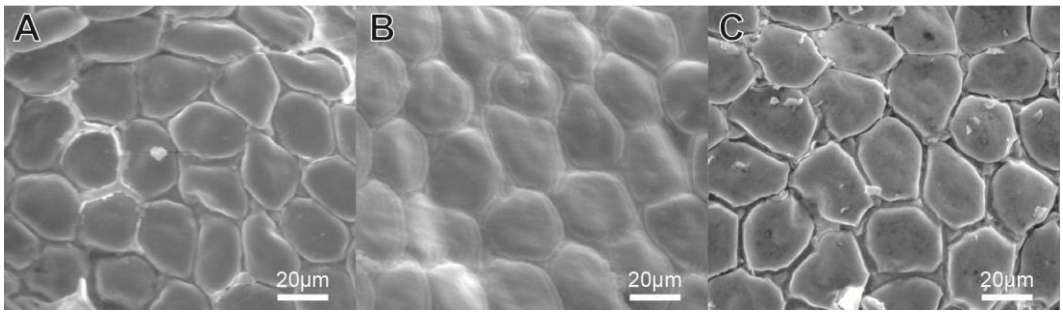

Figure 21. *Pituophis melanoleucus* (A) anterior, (B) middle, and (C) posterior inter-scale keratinocyte images at x1000 magnification.

Counts: 87 90 75

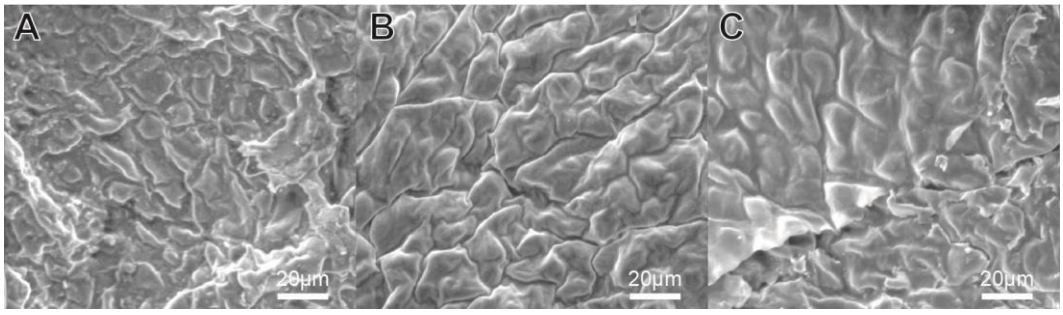

Figure 22. *Python regius* (A) anterior, (B) middle, and (C) posterior inter-scale keratinocyte images at x1000 magnification.

Counts: 163 137 142

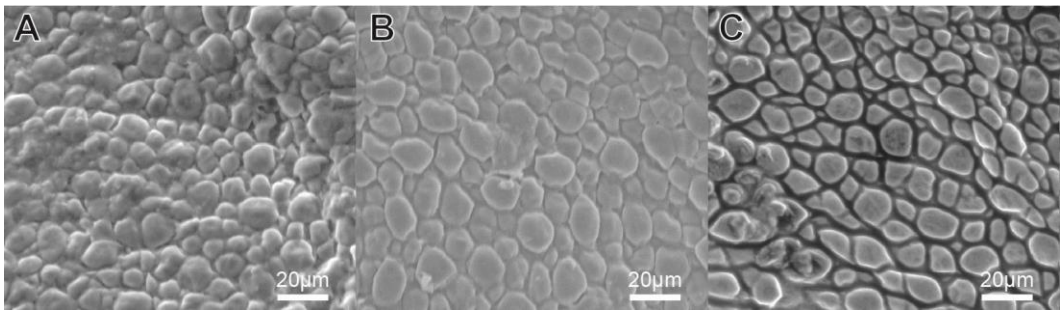

Figure 23. *Nerodia sipedon* (A) anterior, (B) middle, and (C) posterior inter-scale keratinocyte images at x1000 magnification.

Counts: 180 171 164

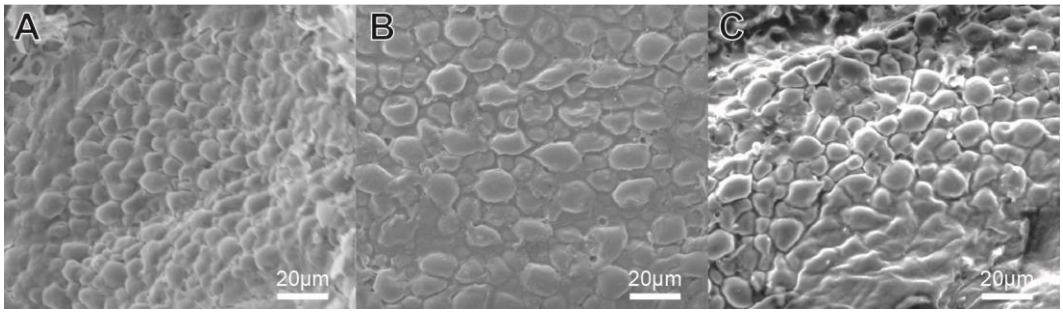

Figure 24. *Liodytes alleni* (A) anterior, (B) middle, and (C) posterior inter-scale keratinocyte images at x1000 magnification.

Counts: 17 20 18

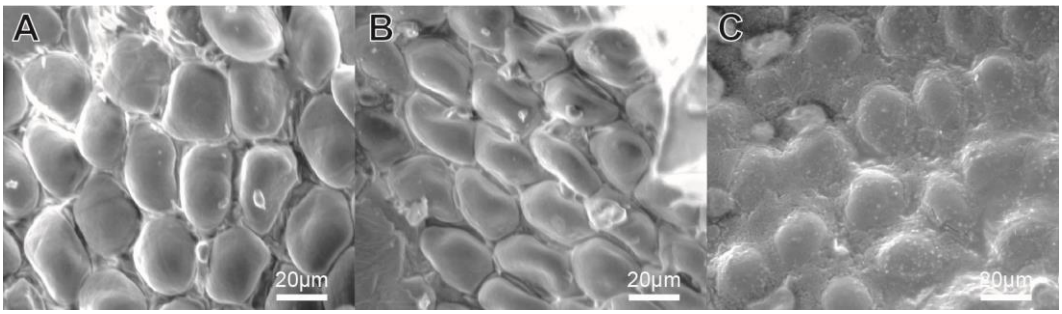

Figure 25. *Rhamphiophis oxyrhynchus* (A) anterior, (B) middle, and (C) posterior inter-scale keratinocyte images at x1000 magnification.

Counts: 583

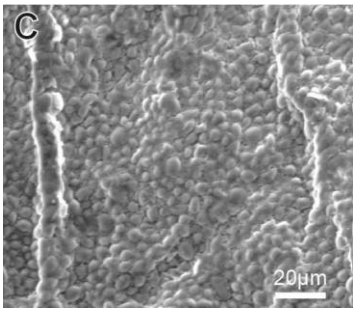

Figure 26. *Xenopeltis unicolor* (C) posterior inter-scale keratinocyte images at x1000 magnification.

DISCUSSION

Tanned Skin for Use in Microstructure Research

We have found that the scale microstructures visible on our tanned specimens are comparable to the published scale microstructures found on shed skin and wet preserved specimens. This means that tanned snakeskins can be used in microstructure research. Tanned snakeskins are much more durable than snake sheds, so they may be kept in long term storage for future study. Tanned skin is also completely dry, removing the need for a dehydration step before SEM unlike wet preserved samples. Tanned skin may be a good alternative to other preservation methods when available for future snake microstructure research, and perhaps other reptile microstructure research.

Scale Microstructure Regional Differences

In general, no major differences were seen between the scale microstructures on the anterior, middle, and posterior dorsal trunk scales. Some regional variations were noted in the *Morelia viridis*, *Ahaetulla nasuta*, and *Liodytes alleni* snake samples. The cell shapes of *Morelia viridis* were elongated in the anterior photo and became more rounded in the middle and posterior photos. The anterior photo of the *Ahaetulla nasuta* the ridges are not well defined and have large spaces between them. The middle contains more distinct ridges that are much closer together, and the posterior also contains distinct ridges that

are even more compact than the middle. The middle and posterior photos of *Liodytes alleni* show elongated cells, while the anterior image shows more rounded cells. This means that the shape of microstructures found can vary depending on the place the scale was sampled from, even from trunk scales. The regional variation of microstructures in uropeltid snakes is an adaptation to cause dirt to selectively bind to the tail (Gans and Baic 1977). It is not unreasonable to assume that other snakes would have regional variation as well, as different parts of the snake interact with its surroundings in different ways. Most published research neglects to state precisely where the scale microstructures were found. If this regional variation is common in snakes, the locations of the samples must be described more precisely for accurate comparisons to be made.

Inter-scale Keratinocyte Microstructures

For our quantitative analysis of the inter-scale keratinocytes, we found that the average size of the keratinocytes varies between species. The shape of the keratinocytes was rather round across all studied species, with *Python regius* keratinocytes being slightly more elongated than the rest. The area and circularity of keratinocytes stayed mostly consistent throughout the body regions of the snakes. With more keratinocyte images, statistical tests would be able to determine if the smaller variations seen are significant or not. The length of a snake specimen did not strongly correlate with average keratinocyte size. With

more snake specimens and species, we would be able to tell if keratinocytes are larger on longer snakes or if there is a different variable affecting keratinocyte size. There is still a lot that we do not know about these structures. We have not found studies that focused on these structures. We hypothesize that these structures are largely formed from the keratinocytes of the alpha layer. We are also unsure why the microstructures produced by the oberhautchen layer are not visible here like they are on the scale. Perhaps the oberhautchen layer needs the flat layer provided by the beta layer to produce their microstructures. Perhaps the oberhautchen cells are still producing their microstructures, but they are unrecognizable without the thick beta layer. The hinge region and inter-scale skin is largely covered by the scales, so it is likely that these structures are present due to the layers of the skin as opposed to ecological adaptations, but it is still possible that they have an impact. The incredibly small size of the keratinocytes in the fossorial *Xenopeltis unicolor* snake might aid in its skin's hydrophobicity and dirt repelling, but the large keratinocyte size in the *Rhamphiophis oxyrhynchus*, the other fossorial snake, suggests otherwise.

Limitations of this Study

Our sample size is relatively small. We were limited by the number of tanned skins we had in our collection and by what snakes we were getting for our other research projects. We only examined the skin of a single individual in all

our species. Further research could focus on sampling multiple specimens in a single species to understand intraspecific variability and factors that may relate to it such as sex, ontogeny, and size.

We are new to using Scanning Electron Microscopes, so much of our time was spent learning how to use the machine and achieve quality images. Some images that made it into our results were taken during that learning process, so they are not as clear as we would have liked. Our FEI Quanta 200™ SEM is also on the older side and was having trouble achieving a high vacuum. Some of the samples had troubles with arcing, and there were other unknown visual glitches.

There are no quantification methods available to examine the nature of the microstructures themselves, a challenge that we originally thought we would solve in this thesis. It quickly became apparent that the variation is too wide and further research is needed to understand how different structures are formed by the oberhautchen cells.

Conclusion

The microstructures of snakeskin are highly variable across species and these differences seem more correlated with phylogeny than ecology, though ecology is also clearly important. Here we showed that tanned skins provide a long lasting and safe alternative to other preservation methods to examine microstructures in SEM. We also showed that in some species there is clear

regional variation in scale microstructures, and therefore future studies should specify the region of the snake sampled. Finally, we described the variation in keratinocytes found in the hinge region of the snakeskin. These structures seem to not have been previously examined deeply in snakes, and they appear to be highly variable across species in size and potentially circularity, but largely consistent between body regions. More research is needed to determine the nature and potential function of these structures.

APPENDIX

Table 1. List of studied snake specimens. *Indicates headless snake specimen, true SVL is longer than the recorded measurement

Specimen ID	Species	Sex	Snout to Vent Length (mm)	Ecology
AHNA001F	*Ahaetulla nasuta*	F	860	Arboreal
MOVI001M	*Morelia viridis*	M	>1290*	Arboreal
PIME001F	*Pituophis melanoleucus*	F	>1441*	Terrestrial
PYRE002F	*Python regius*	F	>950*	Terrestrial
NESI200M	*Nerodia sipedon*	M	566	Aquatic
LIAL002F	*Liodytes alleni*	F	508	Aquatic
RHOX001M	*Rhamphiophis oxyrhynchus*	M	843	Fossorial
XEUN005M	*Xenopeltis unicolor*	M	1021	Fossorial

Table 2. Inter-scale keratinocyte measurements, *Ahaetulla nasuta*

Ahaetulla nasuta Keratinocytes						
Region	**Area (μ^2)**	**Circularity**		**Region**	**Area (μ^2)**	**Circularity**
Anterior	165.895	0.718		Middle	129.919	0.769
Anterior	35.417	0.732		Middle	138.387	0.6
Anterior	13.677	0.809		Middle	81.964	0.754
Anterior	44.117	0.731		Middle	56.983	0.873
Anterior	137.153	0.852		Middle	35.32	0.856
Anterior	36.323	0.752		Middle	29.012	0.706
Anterior	81.211	0.62		Middle	169.907	0.658
Anterior	78.8	0.743		Middle	115.799	0.569
Anterior	134.491	0.915		Middle	82.427	0.543
Anterior	42.13	0.531		Middle	191.416	0.47
Anterior	110.127	0.777		Middle	181.906	0.594
Anterior	173.515	0.612		Middle	126.601	0.677
Anterior	12.114	0.725		Middle	41.435	0.756
Anterior	110.918	0.757		Middle	29.128	0.556
Anterior	116.59	0.951		Posterior	129.707	0.687
Anterior	224.306	0.902		Posterior	120.853	0.573
Anterior	75.212	0.886		Posterior	48.264	0.414
Anterior	12.809	0.88		Posterior	38.927	0.508
Anterior	75.367	0.747		Posterior	100.328	0.631
Middle	89.757	0.696		Posterior	146.952	0.728
Middle	55.266	0.885		Posterior	88.465	0.7
Middle	111.902	0.799		Posterior	90.953	0.783
Middle	36.516	0.787		Posterior	26.91	0.529
Middle	36.69	0.874		Posterior	58.951	0.372
Middle	46.586	0.46				

Table 3. Inter-scale keratinocyte measurements, *Morelia viridis*

Morelia viridis Keratinocytes						
Region	**Area (μ^2)**	**Circularity**		**Region**	**Area (μ^2)**	**Circularity**
Anterior	111.574	0.886		Middle	37.133	0.763
Anterior	68.441	0.712		Middle	46.971	0.526
Anterior	103.839	0.913		Posterior	93.364	0.565
Anterior	25.675	0.878		Posterior	71.933	0.876
Anterior	37.288	0.856		Posterior	64.583	0.601
Anterior	41.069	0.794		Posterior	59.047	0.884
Anterior	47.647	0.75		Posterior	97.84	0.74
Anterior	81.867	0.728		Posterior	112.249	0.65
Anterior	50.077	0.832		Posterior	85.262	0.805
Anterior	26.736	0.648		Posterior	74.498	0.781
Anterior	27.72	0.747		Posterior	221.547	0.873
Anterior	26.312	0.772		Posterior	89.641	0.903
Anterior	93.383	0.714		Posterior	59.279	0.822
Anterior	44.83	0.597		Posterior	43.634	0.78
Anterior	139.815	0.713				
Anterior	76.813	0.868				
Anterior	15.567	0.645				
Middle	100.791	0.839				
Middle	85.204	0.87				
Middle	166.223	0.674				
Middle	105.247	0.932				
Middle	43.364	0.845				
Middle	111.208	0.814				
Middle	94.83	0.76				
Middle	56.848	0.866				

Table 4. Inter-scale keratinocyte measurements, *Pituophis melanoleucus*

Pituophis melanoleucus Keratinocytes						
Region	**Area (μ^2)**	**Circularity**		**Region**	**Area (μ^2)**	**Circularity**
Anterior	512.056	0.857				
Anterior	475.135	0.65				
Anterior	612.809	0.915				
Anterior	555.671	0.805				
Anterior	394.599	0.7				
Anterior	494.387	0.879				
Middle	761.227	0.914				
Middle	800.694	0.845				
Middle	625.212	0.923				
Posterior	656.597	0.854				
Posterior	676.157	0.855				
Posterior	643.924	0.759				
Posterior	555.999	0.832				

Table 5. Inter-scale keratinocyte measurements, *Python regius*

Python regius Keratinocytes						
Region	**Area (μ^2)**	**Circularity**		**Region**	**Area (μ^2)**	**Circularity**
Anterior	93.576	0.854		Middle	240.567	0.624
Anterior	86.053	0.404		Posterior	151.524	0.652
Anterior	97.782	0.455		Posterior	161.458	0.772
Anterior	105.266	0.343		Posterior	150.559	0.449
Anterior	117.535	0.555		Posterior	234.24	0.751
Anterior	155.999	0.78		Posterior	98.052	0.468
Anterior	124.595	0.397		Posterior	194.676	0.725
Anterior	78.569	0.58		Posterior	86.902	0.712
Anterior	66.358	0.82				
Anterior	61.42	0.529				
Middle	145.853	0.637				
Middle	217.921	0.632				
Middle	144.039	0.89				
Middle	97.164	0.695				
Middle	124.248	0.63				
Middle	59.163	0.558				
Middle	86.015	0.721				
Middle	78.935	0.804				
Middle	113.407	0.727				
Middle	63.04	0.666				
Middle	64.545	0.883				
Middle	52.971	0.526				
Middle	75.791	0.583				
Middle	15.664	0.714				

Table 6. Inter-scale keratinocyte measurements, *Nerodia sipedon*

Nerodia sipedon Keratinocytes						
Region	**Area (μ^2)**	**Circularity**		**Region**	**Area (μ^2)**	**Circularity**
Anterior	147.126	0.873		Middle	186.304	0.92
Anterior	146.817	0.942		Middle	84.799	0.814
Anterior	71.412	0.915		Middle	80.652	0.76
Anterior	189.776	0.929		Middle	106.636	0.857
Anterior	85.571	0.911		Middle	107.157	0.855
Anterior	140.664	0.921		Middle	152.643	0.842
Anterior	50.463	0.914		Middle	71.933	0.846
Anterior	55.729	0.903		Posterior	91.262	0.688
Anterior	35.34	0.68		Posterior	143.441	0.904
Anterior	154.032	0.942		Posterior	60.822	0.923
Anterior	45.795	0.892		Posterior	158.14	0.887
Anterior	141.377	0.898		Posterior	107.986	0.859
Anterior	42.728	0.864		Posterior	79.051	0.778
Anterior	131.52	0.912		Posterior	108.893	0.825
Anterior	78.665	0.823		Posterior	138.619	0.931
Anterior	121.277	0.888		Posterior	52.353	0.923
Anterior	31.269	0.898		Posterior	143.499	0.868
Anterior	53.472	0.79		Posterior	53.221	0.745
Anterior	62.674	0.93		Posterior	130.941	0.864
Middle	95.062	0.859		Posterior	25.675	0.85
Middle	186.188	0.907				
Middle	81.578	0.835				
Middle	119.078	0.83				
Middle	204.977	0.807				
Middle	43.21	0.847				

Table 7. Inter-scale keratinocyte measurements, *Liodytes alleni*

Liodytes alleni Keratinocytes						
Region	**Area (μ^2)**	**Circularity**		**Region**	**Area (μ^2)**	**Circularity**
Anterior	100.502	0.928		Middle	128.125	0.945
Anterior	35.513	0.873		Middle	41.011	0.923
Anterior	57.407	0.843		Posterior	135.899	0.946
Anterior	47.608	0.898		Posterior	39.911	0.867
Anterior	49.749	0.927		Posterior	106.944	0.859
Anterior	66.319	0.878		Posterior	66.262	0.809
Anterior	48.187	0.834		Posterior	40.509	0.854
Anterior	65.066	0.852		Posterior	46.528	0.925
Anterior	73.881	0.909		Posterior	95.66	0.939
Anterior	24.749	0.701		Posterior	52.855	0.819
Anterior	43.056	0.907		Posterior	15.316	0.759
Anterior	88.773	0.722		Posterior	61.555	0.588
Anterior	36.4	0.923				
Anterior	40.76	0.94				
Middle	59.664	0.89				
Middle	34.24	0.935				
Middle	42.631	0.755				
Middle	88.966	0.904				
Middle	179.398	0.835				
Middle	177.334	0.93				
Middle	188.021	0.76				
Middle	120.737	0.728				
Middle	61.574	0.845				
Middle	40.683	0.934				
Middle	166.319	0.824				

Table 8. Inter-scale keratinocyte measurements, *Rhamphiophis oxyrhynchus*

Rhamphiophis oxyrhynchus Keratinocytes						
Region	**Area (μ^2)**	**Circularity**		**Region**	**Area (μ^2)**	**Circularity**
Anterior	737.442	0.904				
Anterior	628.434	0.879				
Anterior	647.338	0.84				
Anterior	709.626	0.926				
Anterior	502.18	0.858				
Anterior	626.89	0.947				
Middle	528.299	0.668				
Middle	427.431	0.772				
Middle	594.946	0.817				
Middle	552.836	0.825				
Posterior	420.775	0.939				
Posterior	476.254	0.927				
Posterior	557.89	0.945				
Posterior	588.735	0.935				
Posterior	243.75	0.945				

Table 9. Inter-scale keratinocyte measurements, *Xenopeltis unicolor*

Xenopeltis unicolor Keratinocytes						
Region	**Area (μ^2)**	**Circularity**		**Region**	**Area (μ^2)**	**Circularity**
Posterior	18.538	0.867		Posterior	15.22	0.856
Posterior	25.714	0.898		Posterior	14.024	0.884
Posterior	14.333	0.945		Posterior	17.207	0.92
Posterior	17.13	0.938		Posterior	10.166	0.848
Posterior	7.87	0.886		Posterior	15.934	0.901
Posterior	8.14	0.932		Posterior	16.937	0.861
Posterior	10.706	0.93				
Posterior	23.013	0.923				
Posterior	10.59	0.868				
Posterior	23.129	0.805				
Posterior	10.224	0.885				
Posterior	18.229	0.89				
Posterior	12.674	0.883				
Posterior	12.442	0.919				
Posterior	10.571	0.904				
Posterior	13.368	0.92				
Posterior	14.969	0.905				
Posterior	3.742	0.894				
Posterior	6.752	0.88				
Posterior	10.725	0.823				
Posterior	10.108	0.802				
Posterior	18.383	0.889				
Posterior	25.656	0.868				
Posterior	13.407	0.924				
Posterior	14.198	0.922				

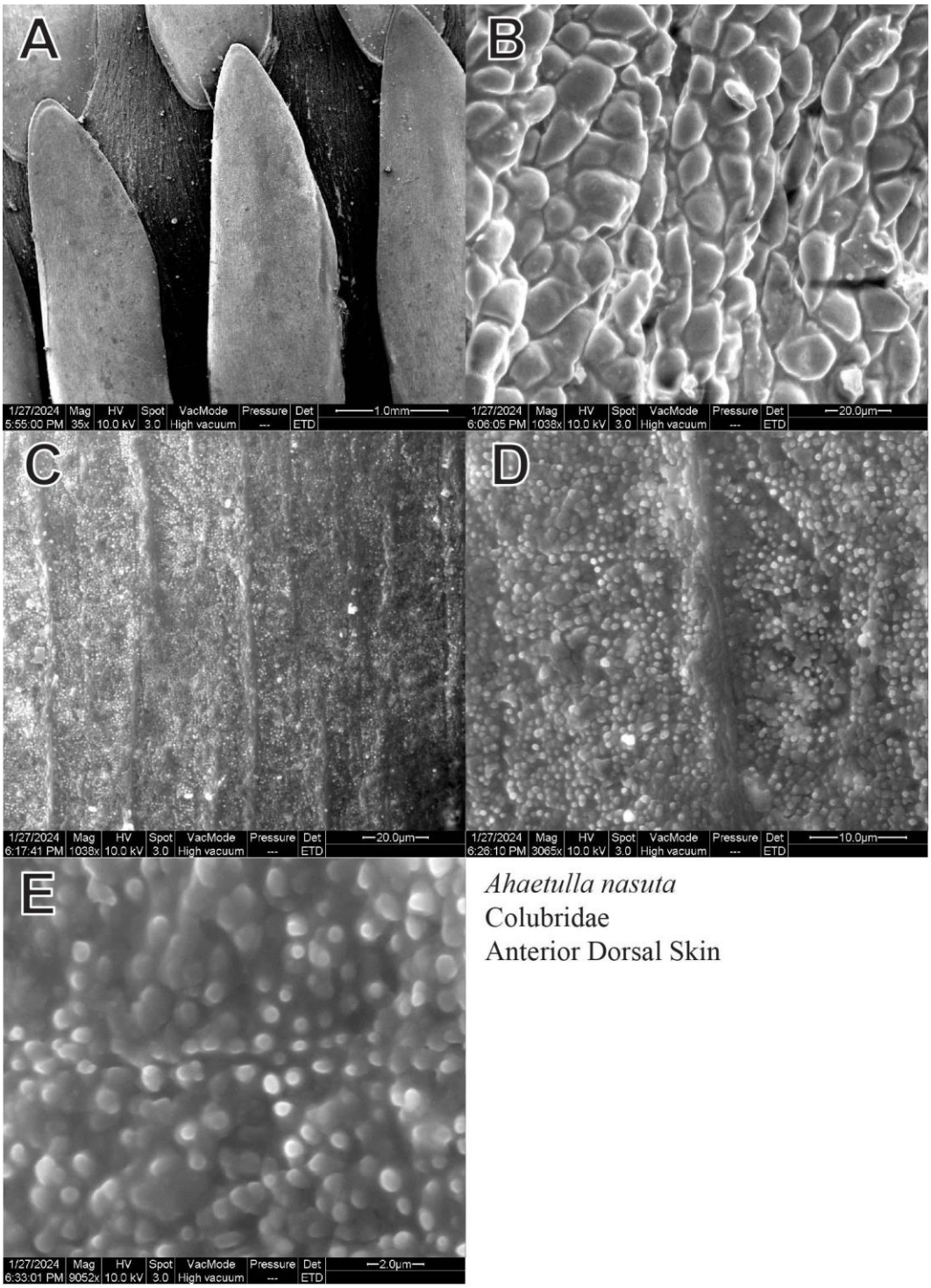

Figure 27. Unedited SEM images of *Ahaetulla nasuta* anterior dorsal snakeskin microstructures. (A) Scale morphology (B) Inter-scale keratinocytes (C-E) Scale microstructures at various levels of magnification

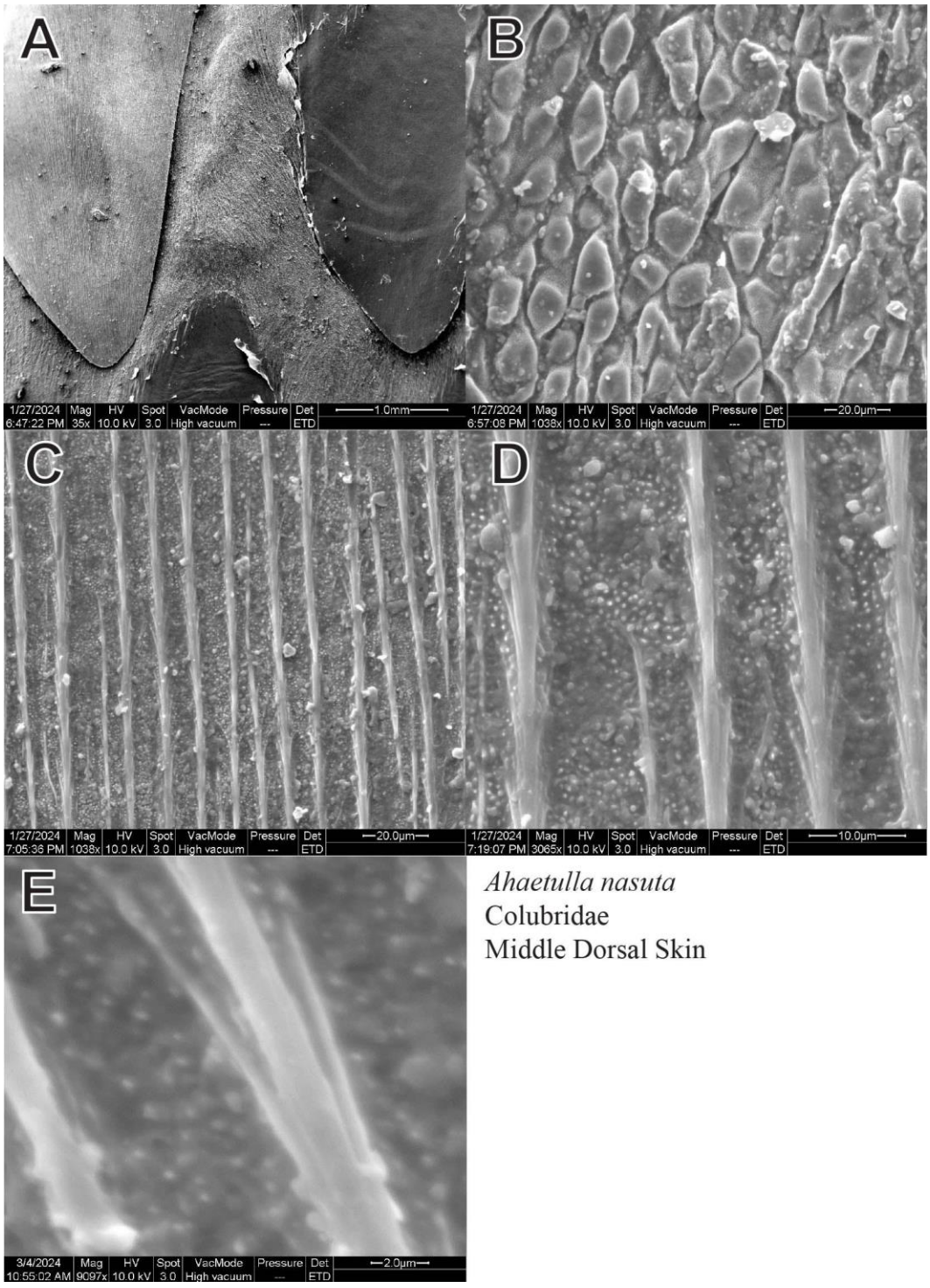

Figure 28. Unedited SEM images of *Ahaetulla nasuta* middle dorsal snakeskin microstructures. (A) Scale morphology (B) Inter-scale keratinocytes (C-E) Scale microstructures at various levels of magnification

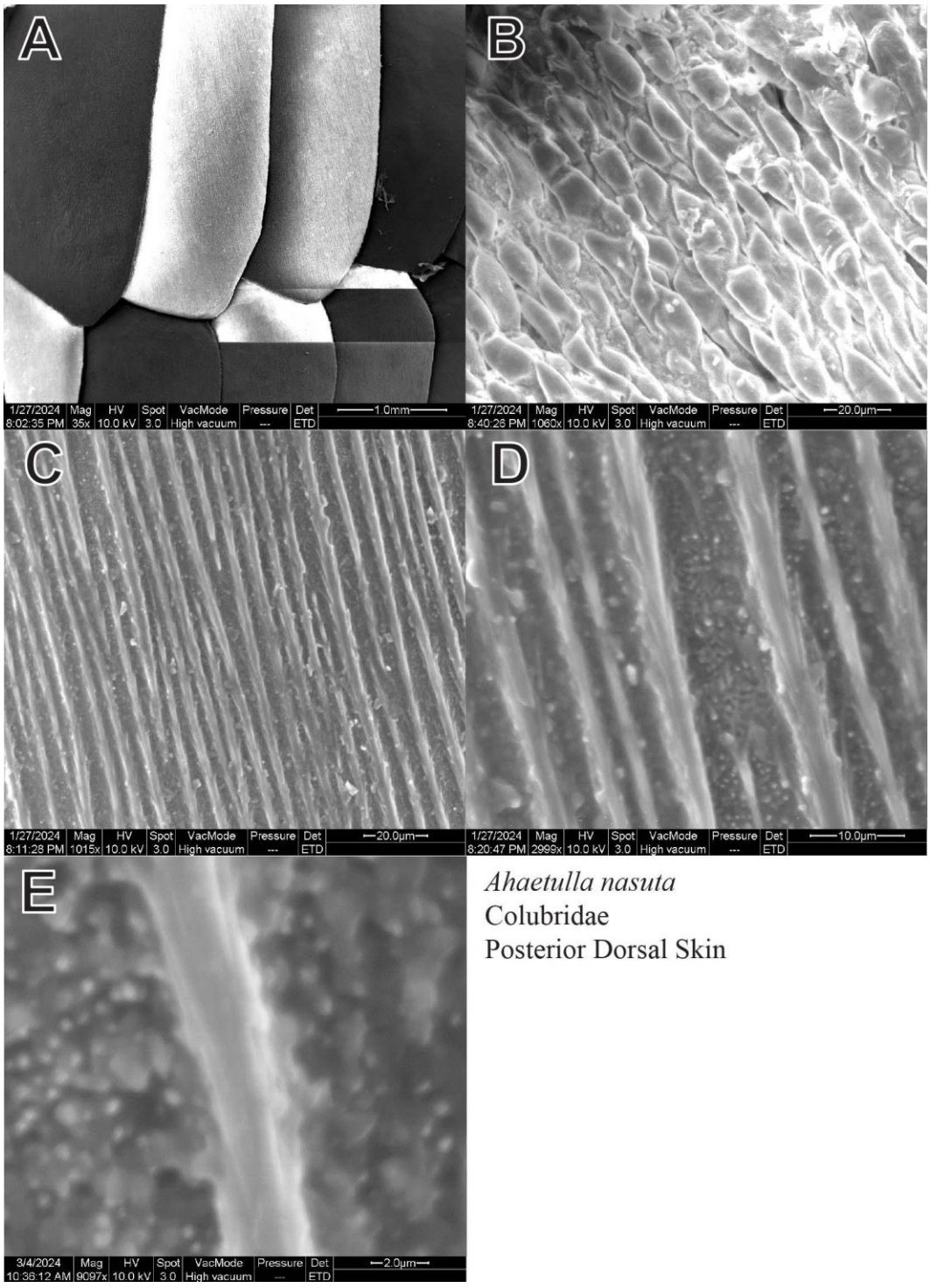

Figure 29. Unedited SEM images of *Ahaetulla nasuta* posterior dorsal snakeskin microstructures. (A) Scale morphology (B) Inter-scale keratinocytes (C-E) Scale microstructures at various levels of magnification

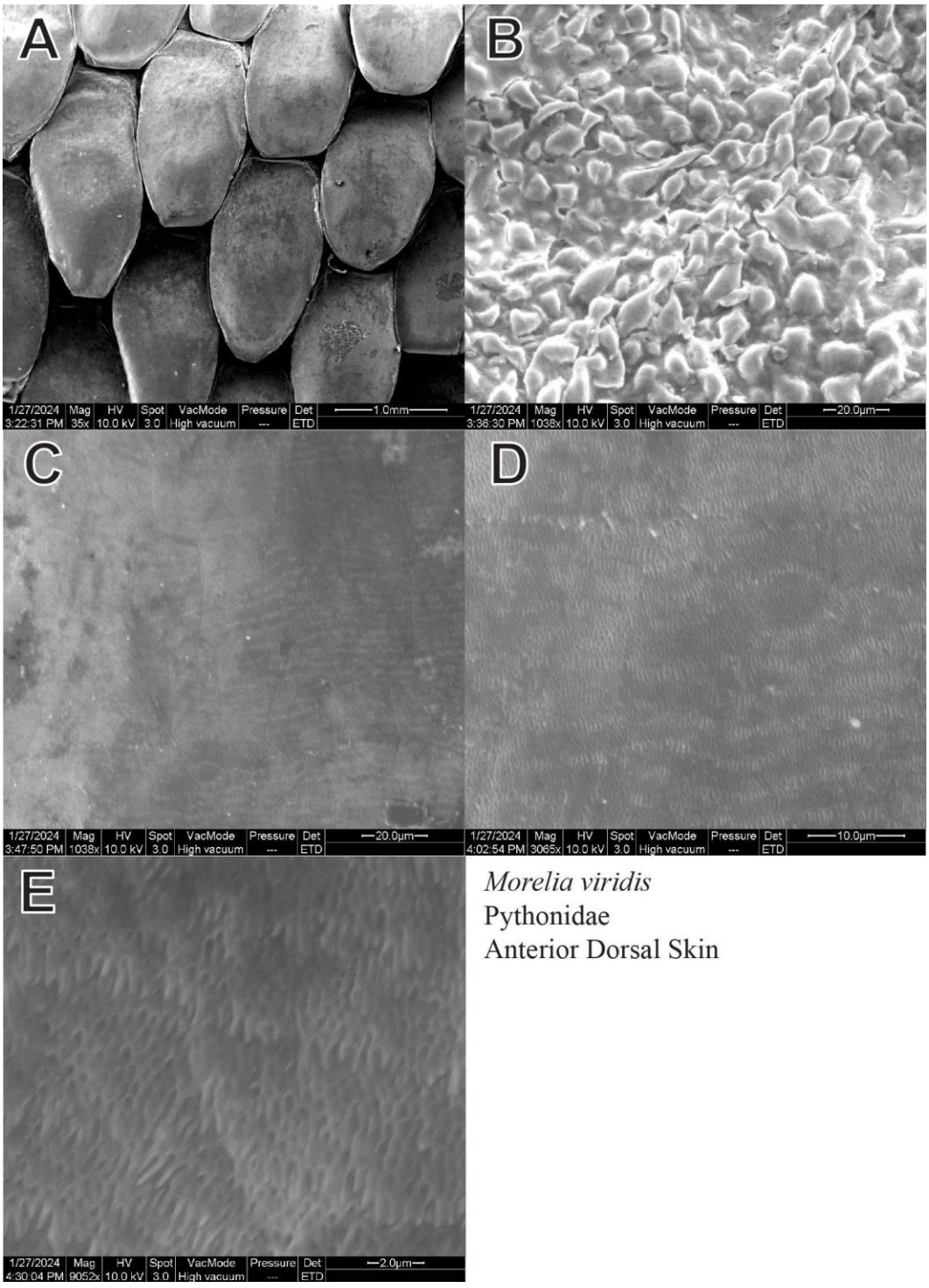

Figure 30. Unedited SEM images of *Morelia viridis* anterior dorsal snakeskin microstructures. (A) Scale morphology (B) Inter-scale keratinocytes (C-E) Scale microstructures at various levels of magnification

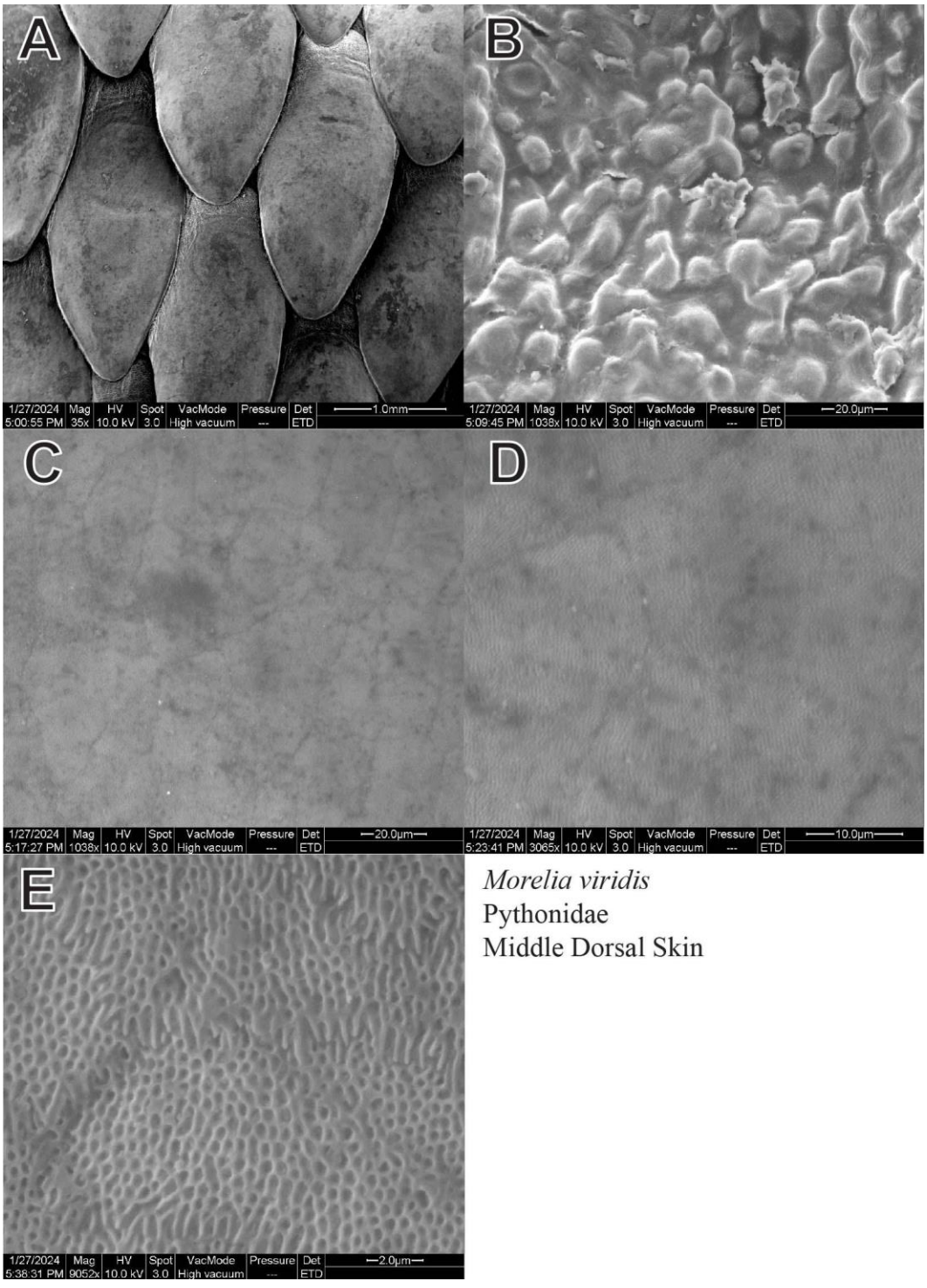

Figure 31. Unedited SEM images of *Morelia viridis* middle dorsal snakeskin microstructures. (A) Scale morphology (B) Inter-scale keratinocytes (C-E) Scale microstructures at various levels of magnification

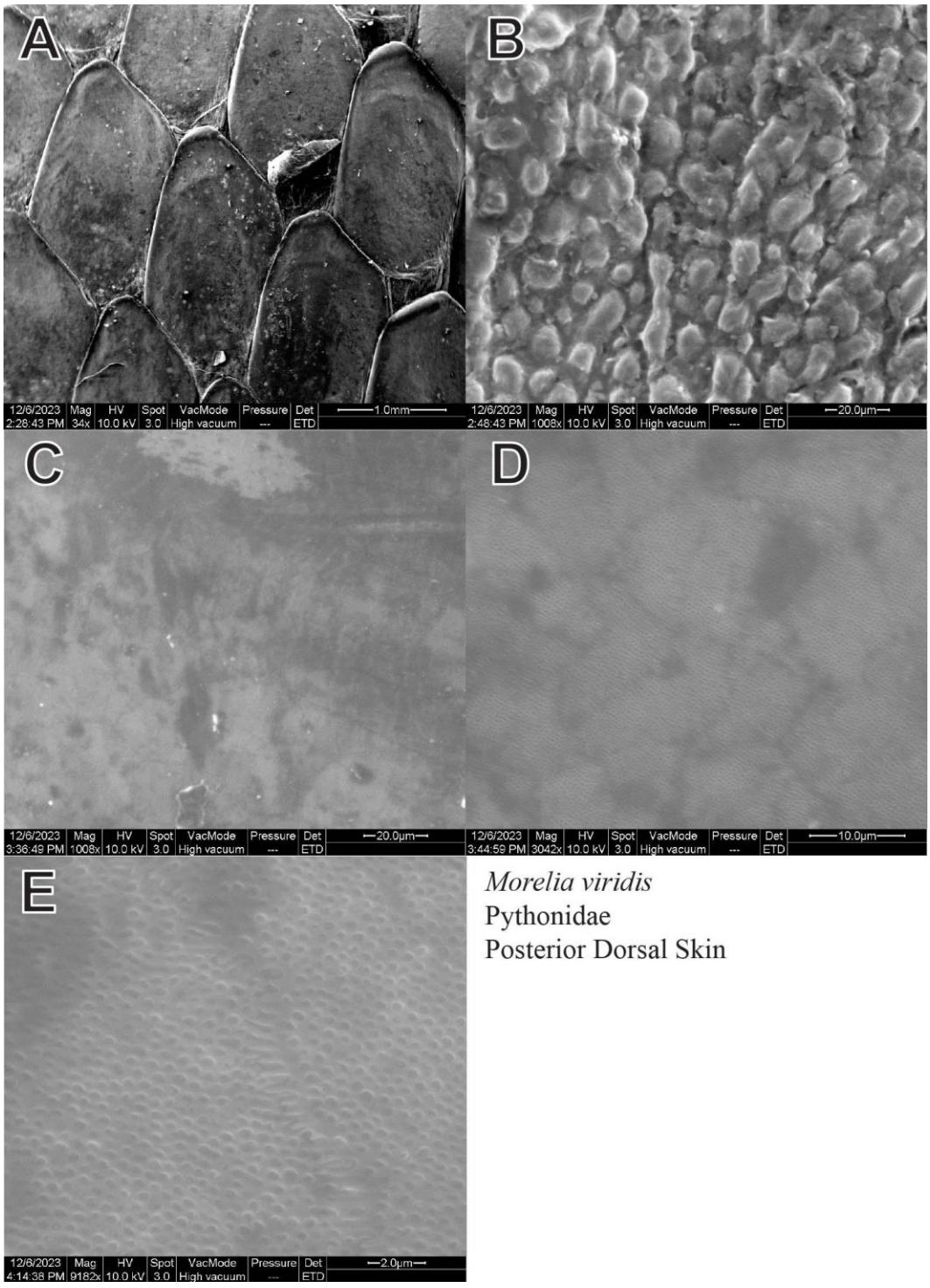

Figure 32. Unedited SEM images of *Morelia viridis* posterior dorsal snakeskin microstructures. (A) Scale morphology (B) Inter-scale keratinocytes (C-E) Scale microstructures at various levels of magnification

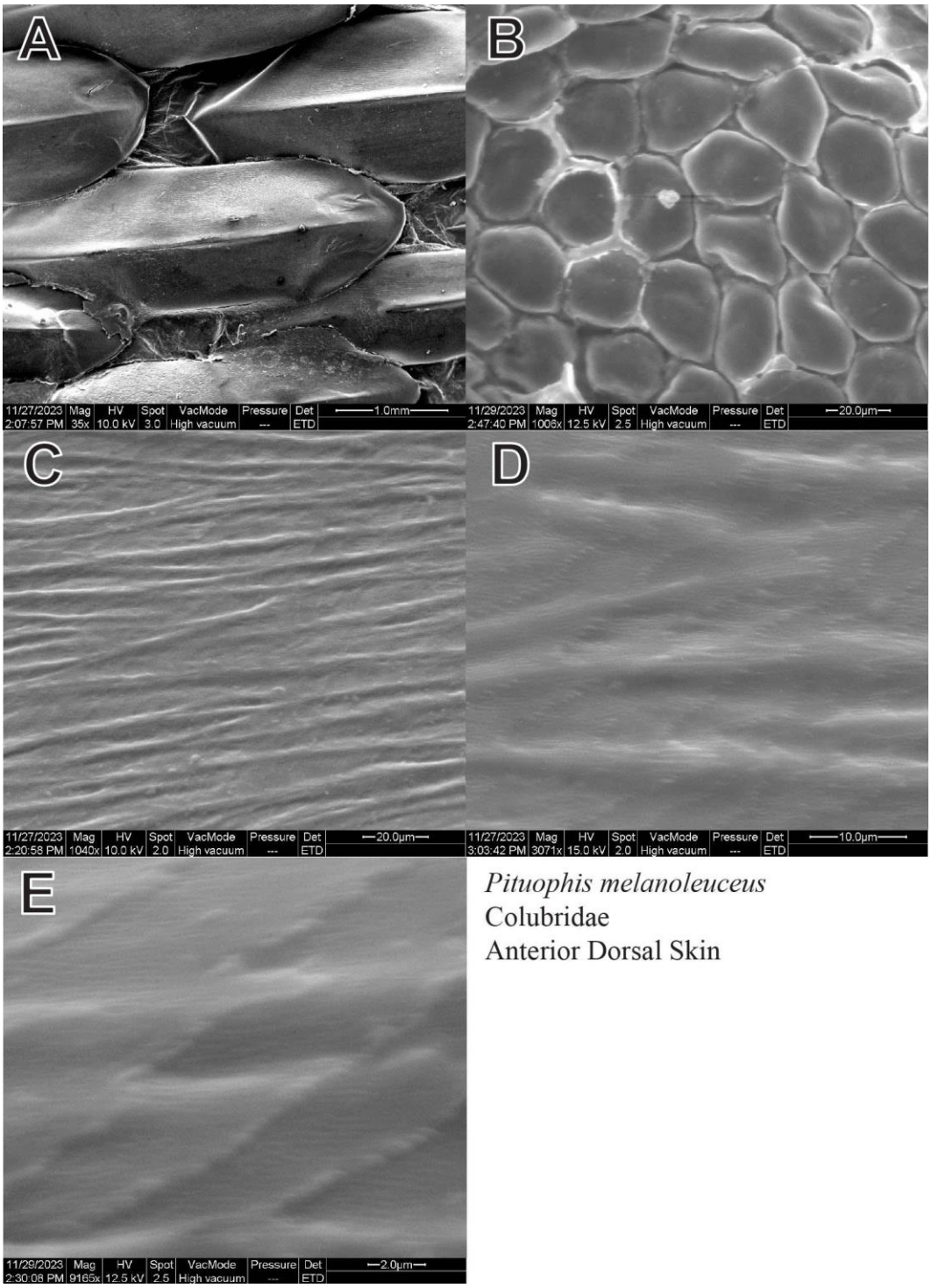

Figure 33. Unedited SEM images of *Pituophis melanoleucus* anterior dorsal snakeskin microstructures. (A) Scale morphology (B) Inter-scale keratinocytes (C-E) Scale microstructures at various levels of magnification

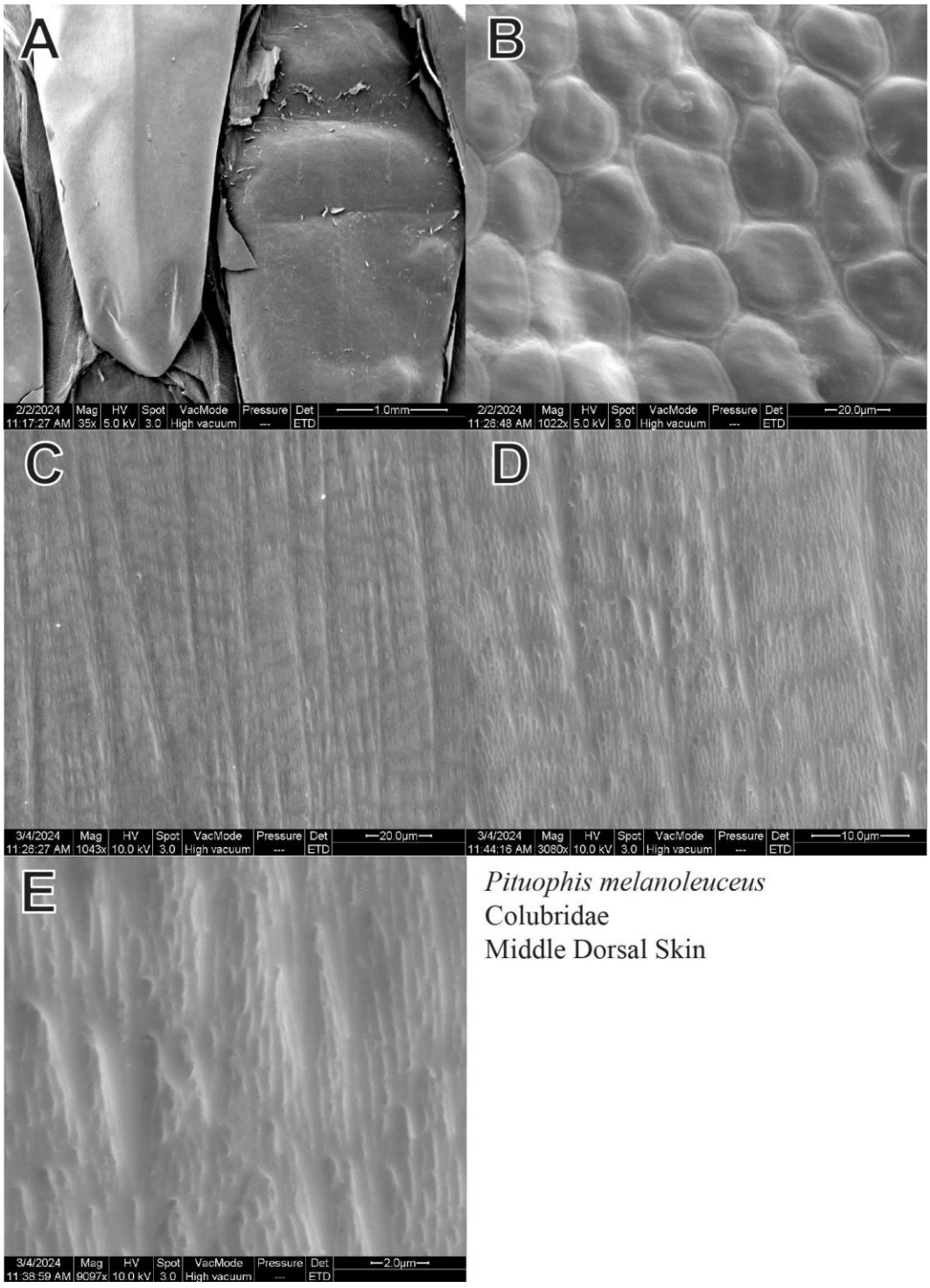

Figure 34. Unedited SEM images of *Pituophis melanoleucus* middle dorsal snakeskin microstructures. (A) Scale morphology (B) Inter-scale keratinocytes (C-E) Scale microstructures at various levels of magnification

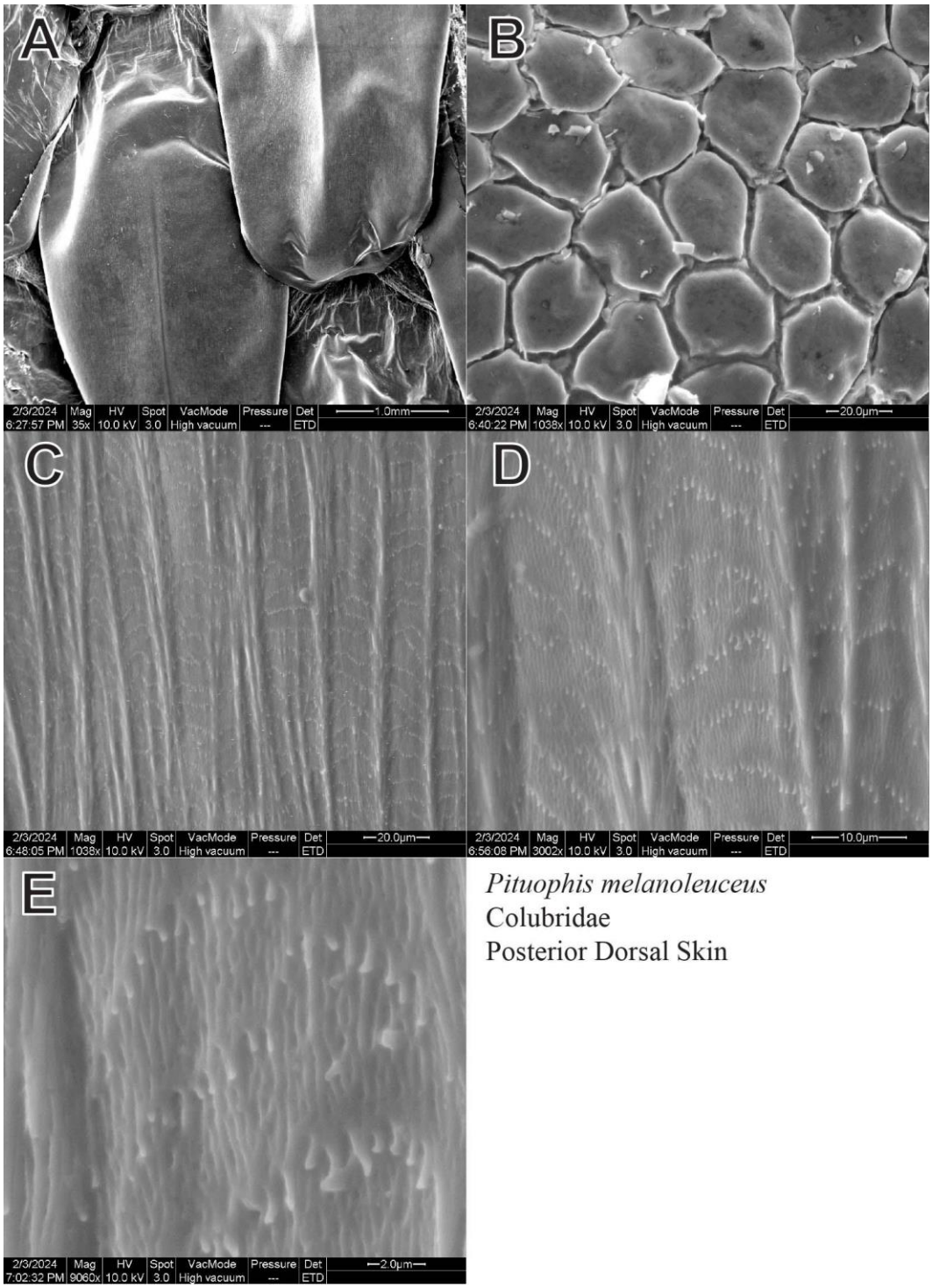

Figure 35. Unedited SEM images of *Pituophis melanoleucus* posterior dorsal snakeskin microstructures. (A) Scale morphology (B) Inter-scale keratinocytes (C-E) Scale microstructures at various levels of magnification

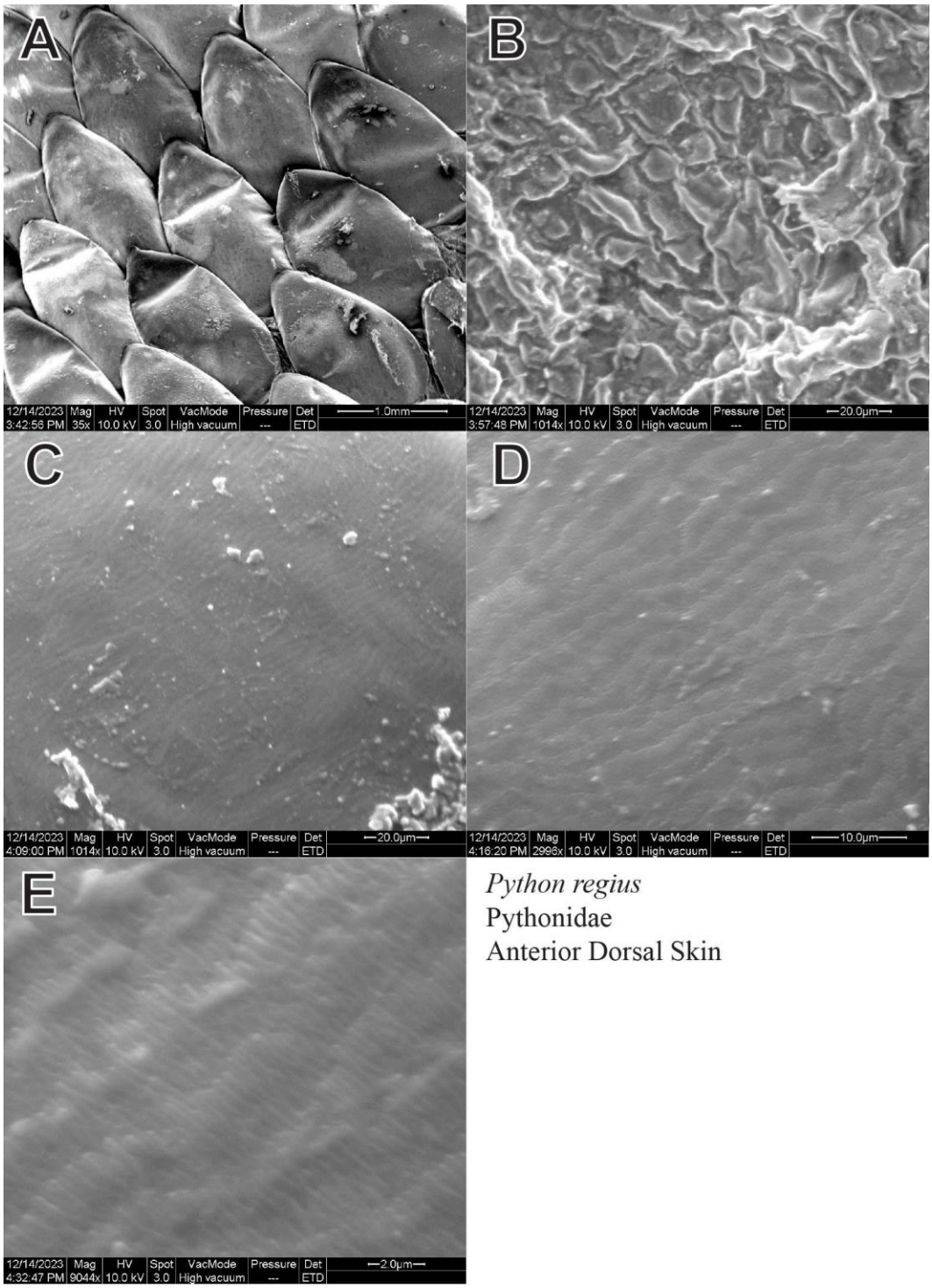

Figure 36. Unedited SEM images of *Python regius* anterior dorsal snakeskin microstructures. (A) Scale morphology (B) Inter-scale keratinocytes (C-E) Scale microstructures at various levels of magnification

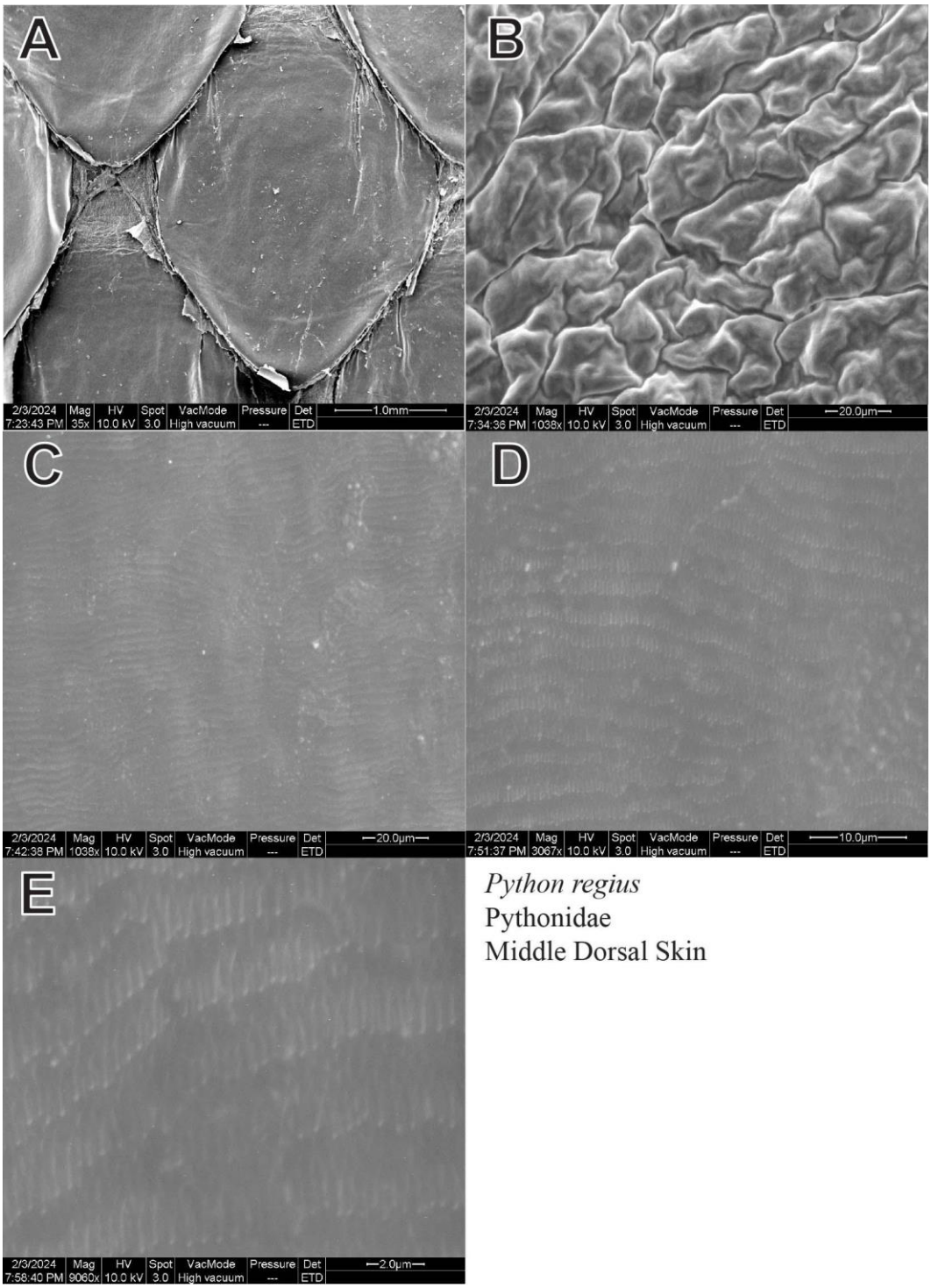

Figure 37. Unedited SEM images of *Python regius* middle dorsal snakeskin microstructures. (A) Scale morphology (B) Inter-scale keratinocytes (C-E) Scale microstructures at various levels of magnification

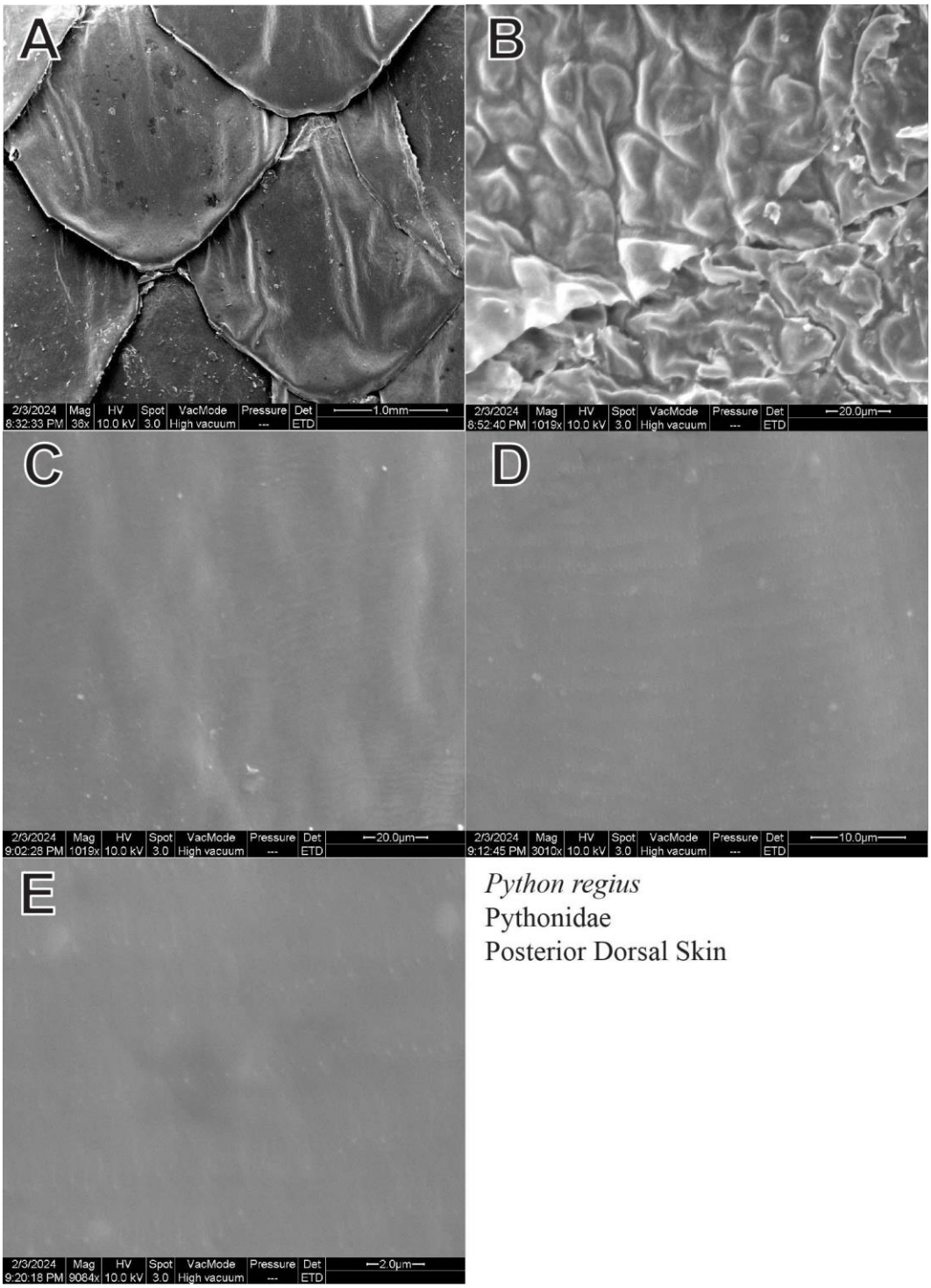

Figure 38. Unedited SEM images of *Python regius* posterior dorsal snakeskin microstructures. (A) Scale morphology (B) Inter-scale keratinocytes (C-E) Scale microstructures at various levels of magnification

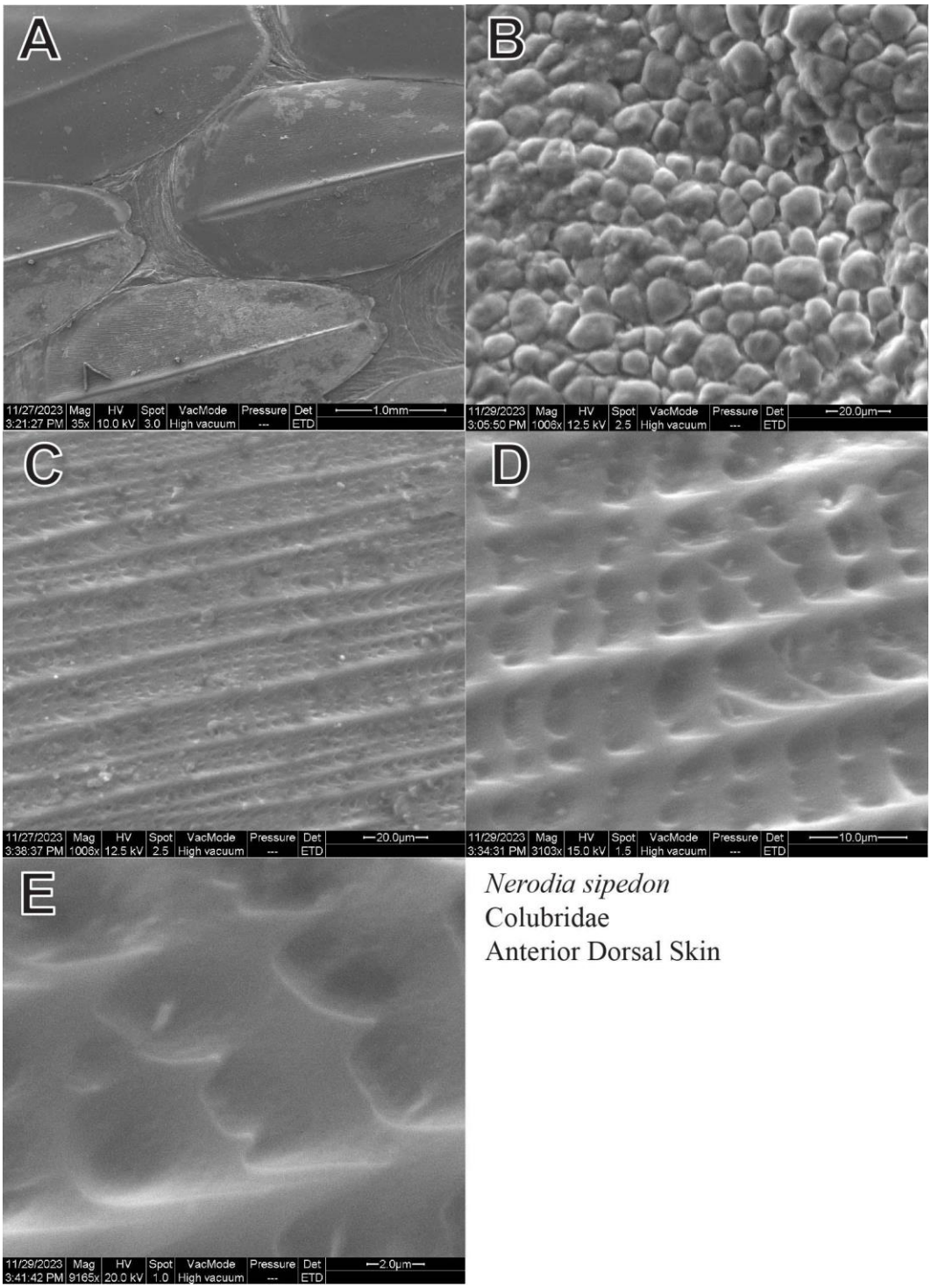

Figure 39. Unedited SEM images of *Nerodia sipedon* anterior dorsal snakeskin microstructures. (A) Scale morphology (B) Inter-scale keratinocytes (C-E) Scale microstructures at various levels of magnification

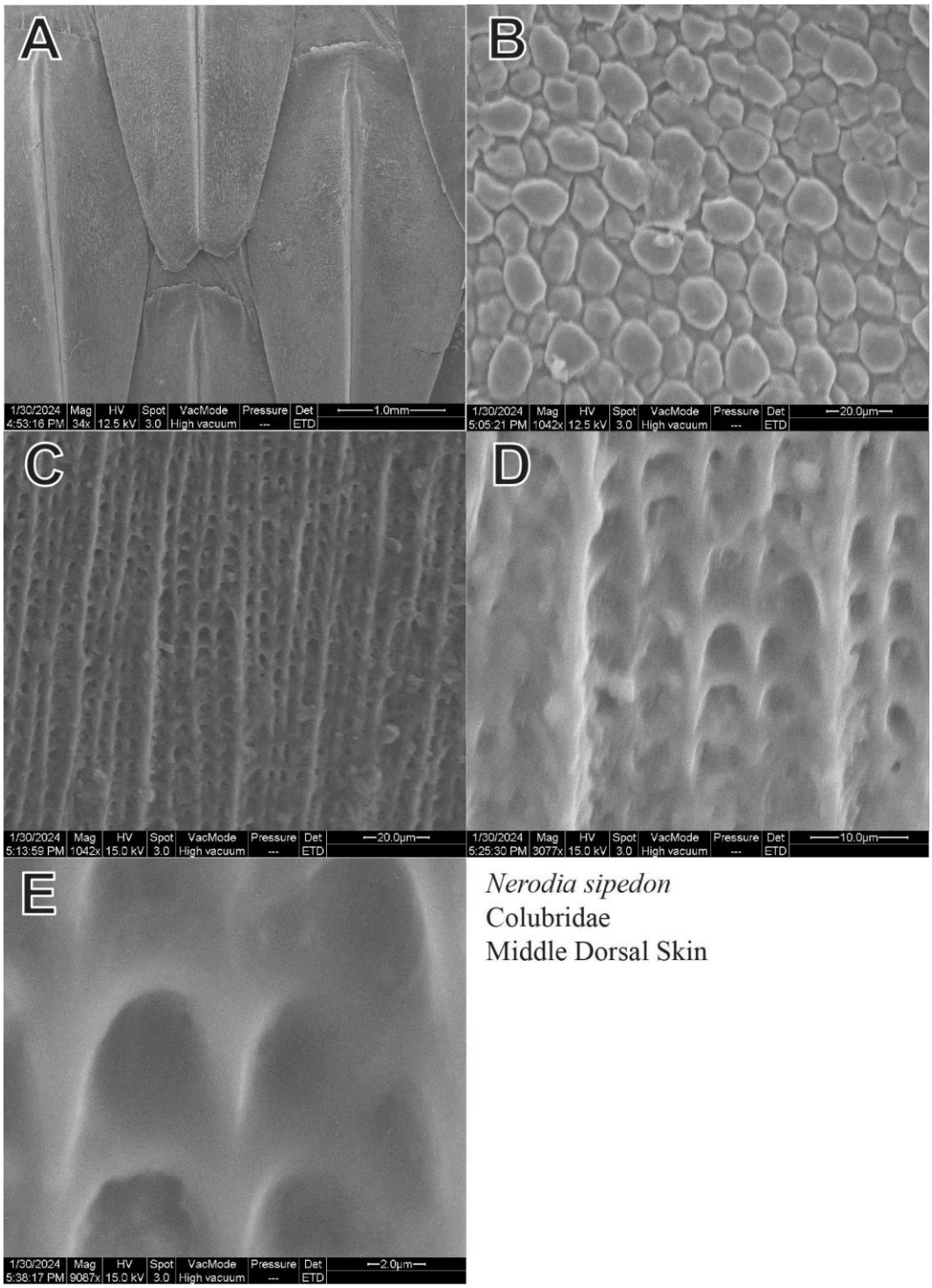

Figure 40. Unedited SEM images of *Nerodia sipedon* middle dorsal snakeskin microstructures. (A) Scale morphology (B) Inter-scale keratinocytes (C-E) Scale microstructures at various levels of magnification

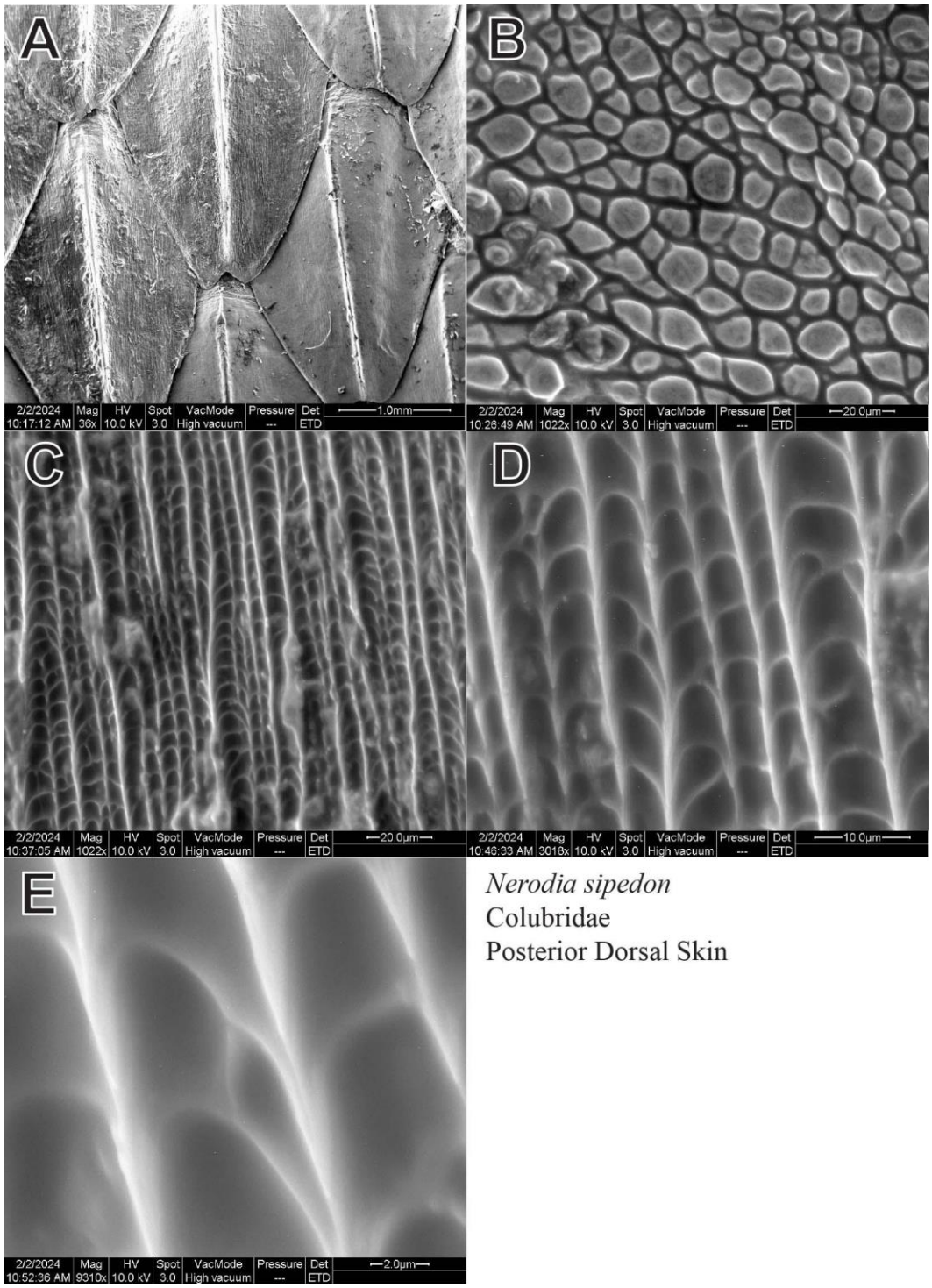

Figure 41. Unedited SEM images of *Nerodia sipedon* posterior dorsal snakeskin microstructures. (A) Scale morphology (B) Inter-scale keratinocytes (C-E) Scale microstructures at various levels of magnification

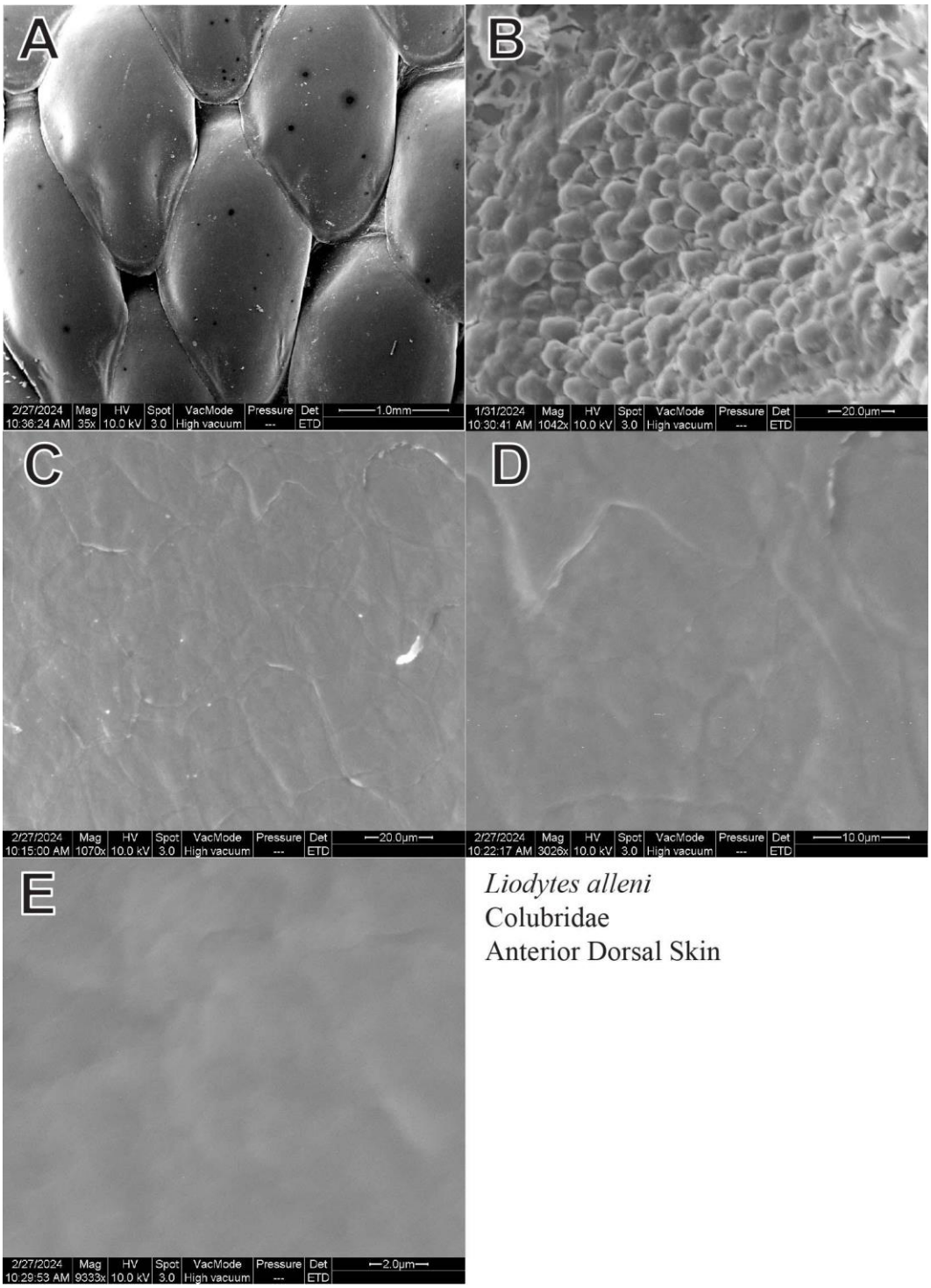

Figure 42. Unedited SEM images of *Liodytes alleni* anterior dorsal snakeskin microstructures. (A) Scale morphology (B) Inter-scale keratinocytes (C-E) Scale microstructures at various levels of magnification

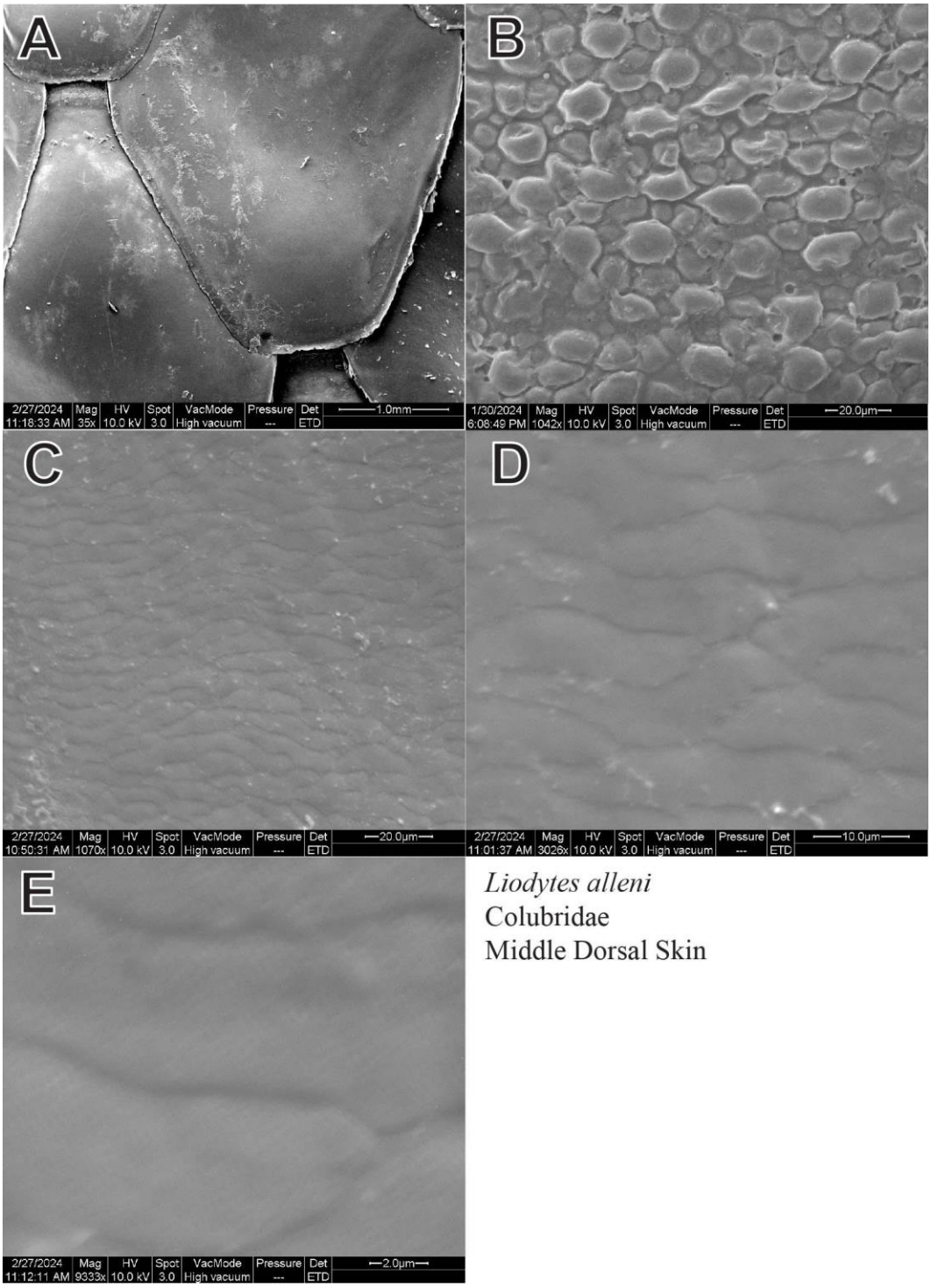

Figure 43. Unedited SEM images of *Liodytes alleni* middle dorsal snakeskin microstructures. (A) Scale morphology (B) Inter-scale keratinocytes (C-E) Scale microstructures at various levels of magnification

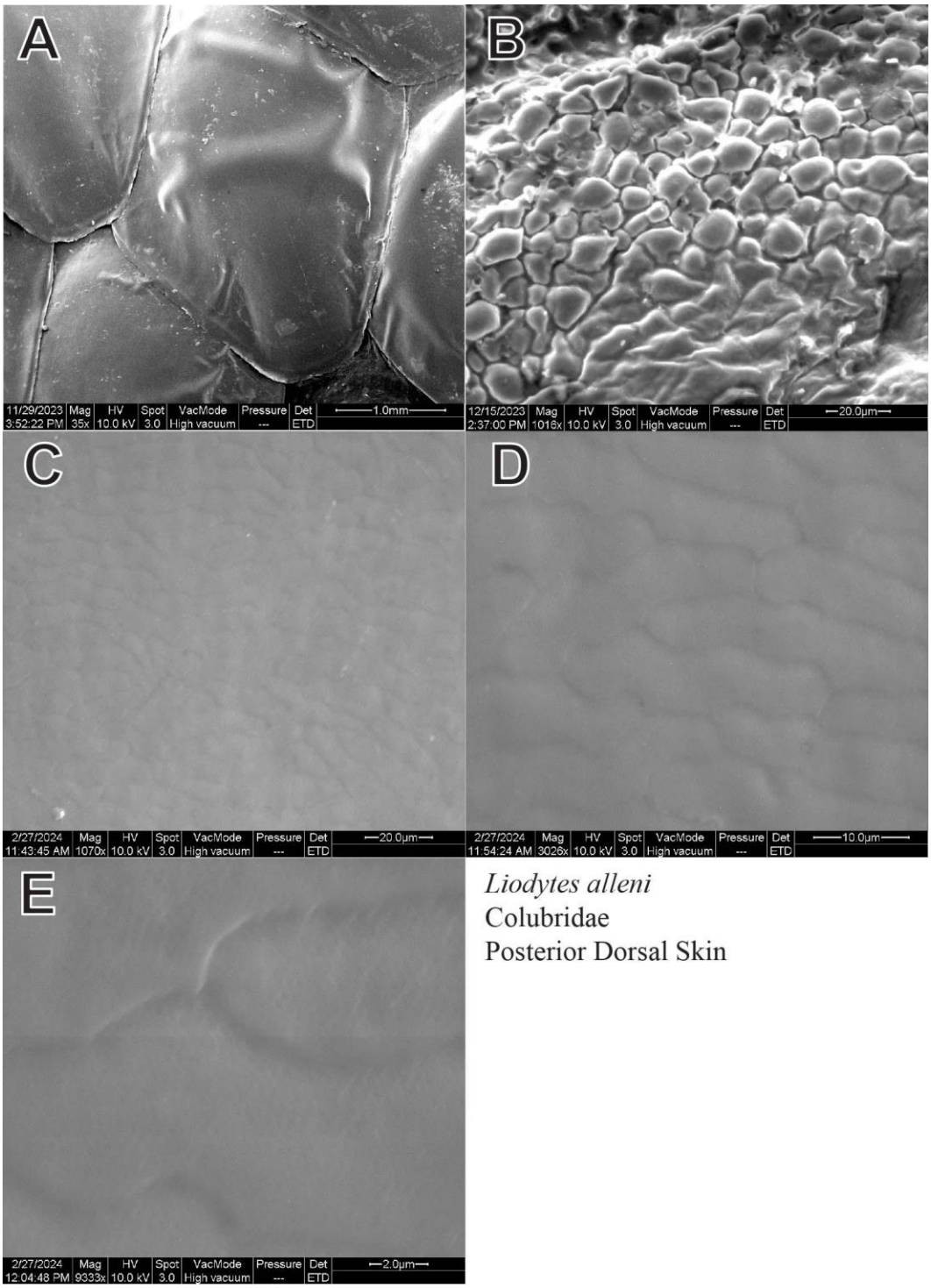

Figure 44. Unedited SEM images of *Liodytes alleni* posterior dorsal snakeskin microstructures. (A) Scale morphology (B) Inter-scale keratinocytes (C-E) Scale microstructures at various levels of magnification

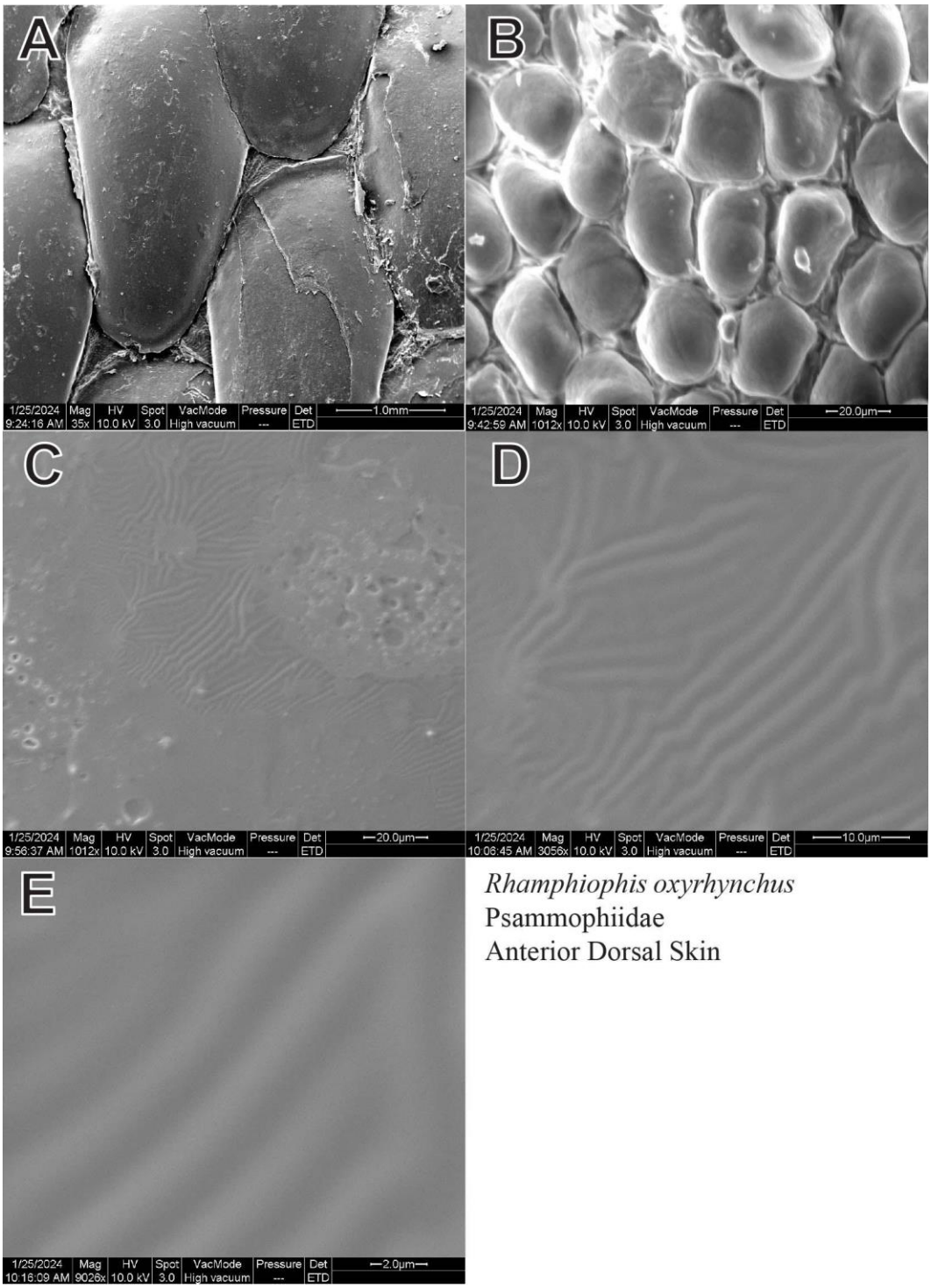

Figure 45. Unedited SEM images of *Rhamphiophis oxyrhynchus* anterior dorsal snakeskin microstructures. (A) Scale morphology (B) Inter-scale keratinocytes (C-E) Scale microstructures at various levels of magnification

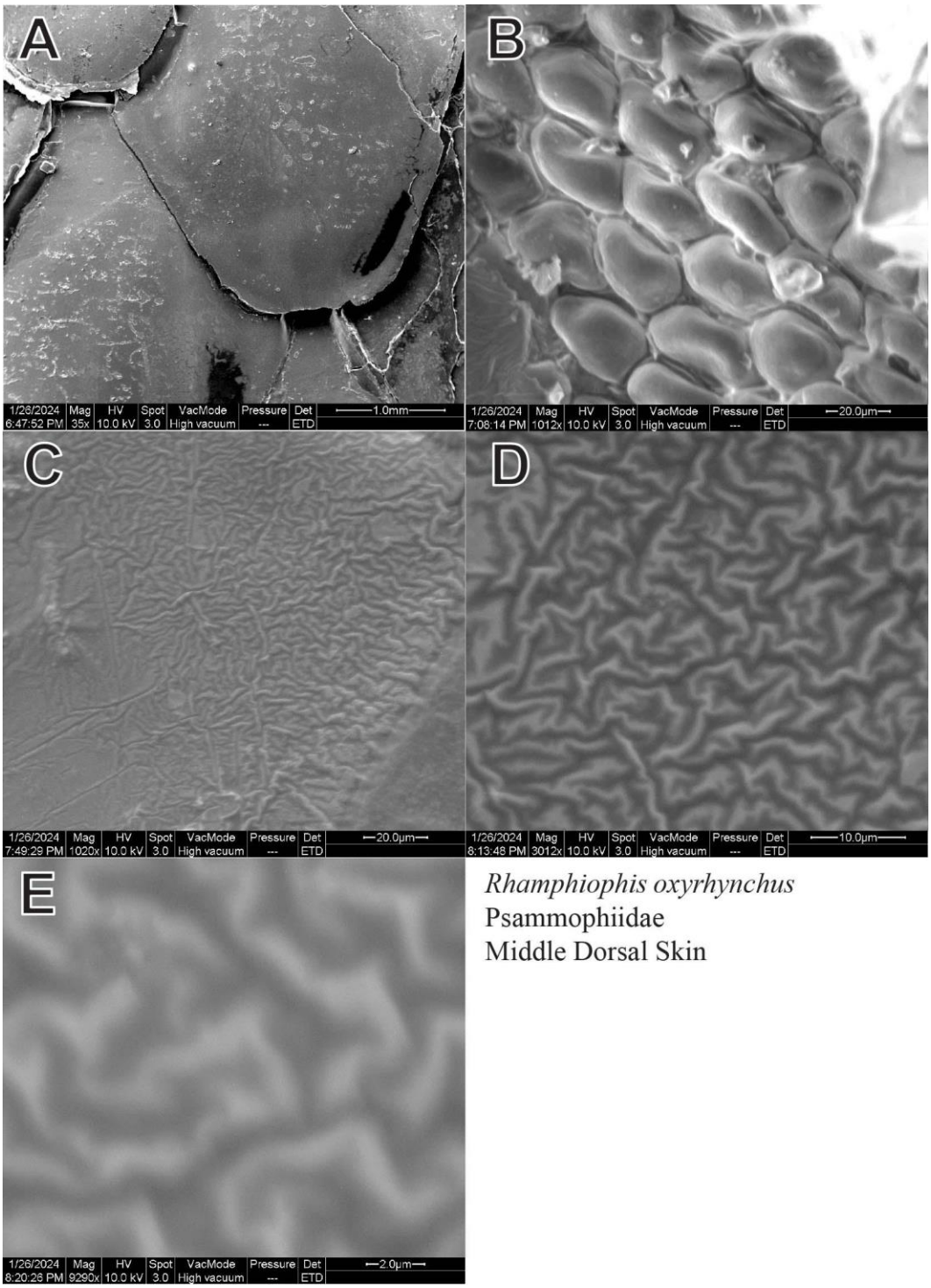

Figure 46. Unedited SEM images of *Rhamphiophis oxyrhynchus* middle dorsal snakeskin microstructures. (A) Scale morphology (B) Inter-scale keratinocytes (C-E) Scale microstructures at various levels of magnification

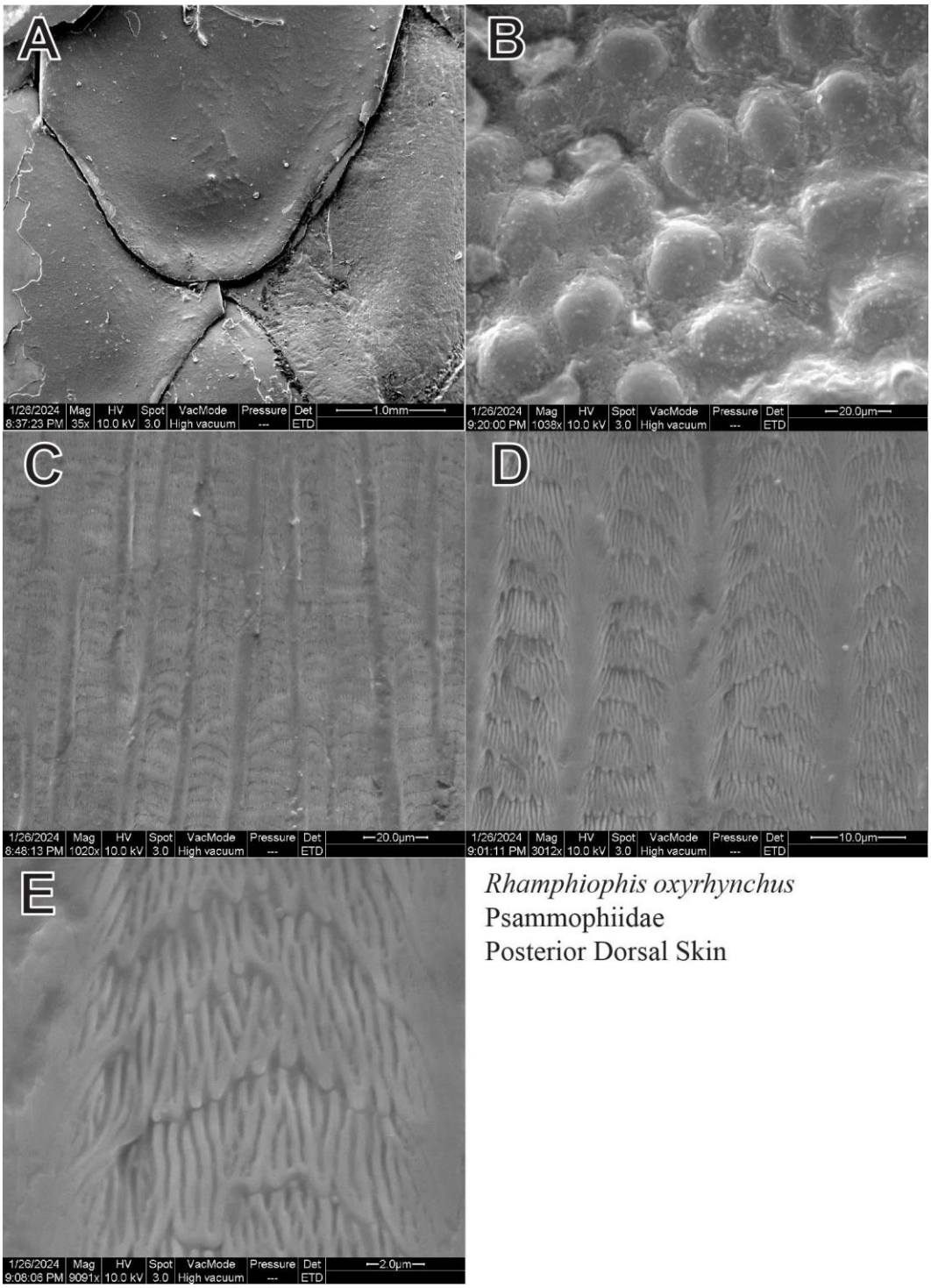

Figure 47. Unedited SEM images of *Rhamphiophis oxyrhynchus* posterior dorsal snakeskin microstructures. (A) Scale morphology (B) Inter-scale keratinocytes (C-E) Scale microstructures at various levels of magnification

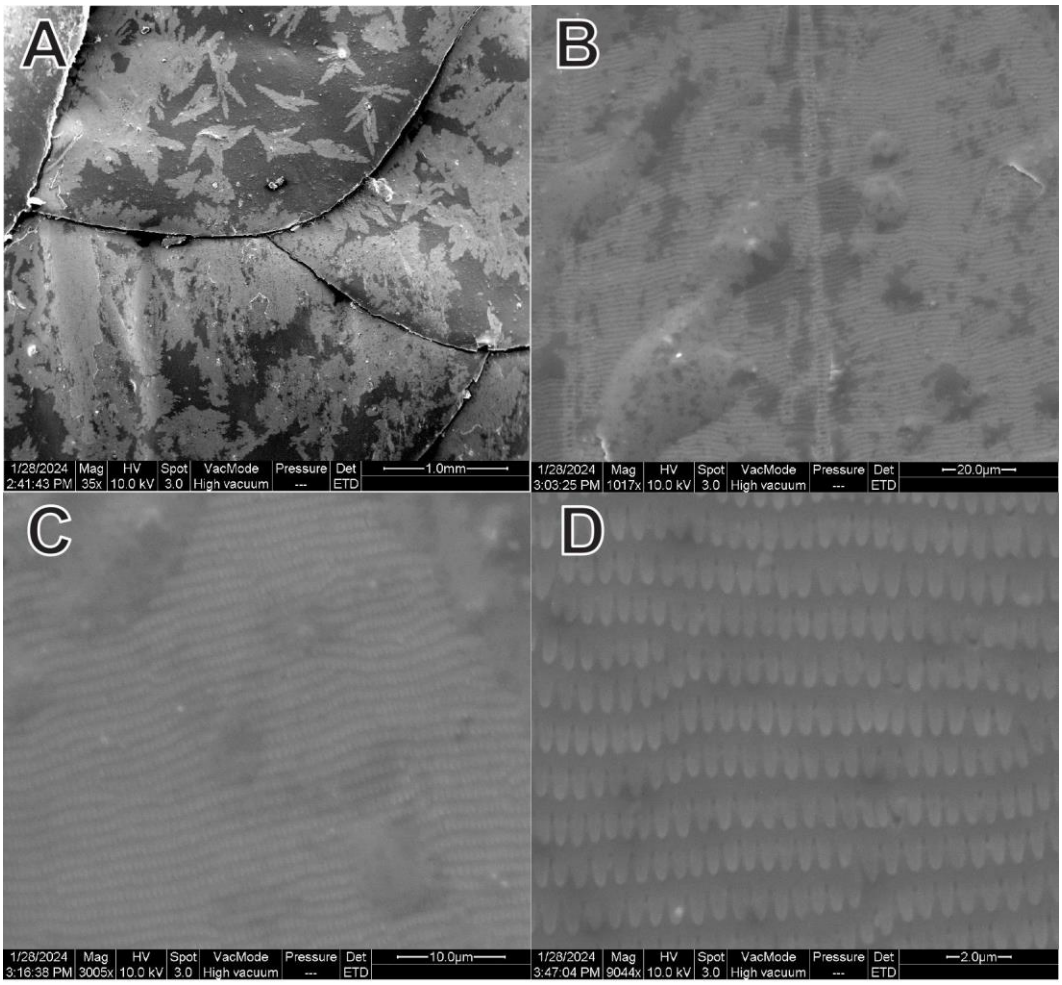

Figure 48. Unedited SEM images of *Xenopeltis unicolor* anterior dorsal snakeskin microstructures. (A) Scale morphology (B-D) Scale microstructures at various levels of magnification

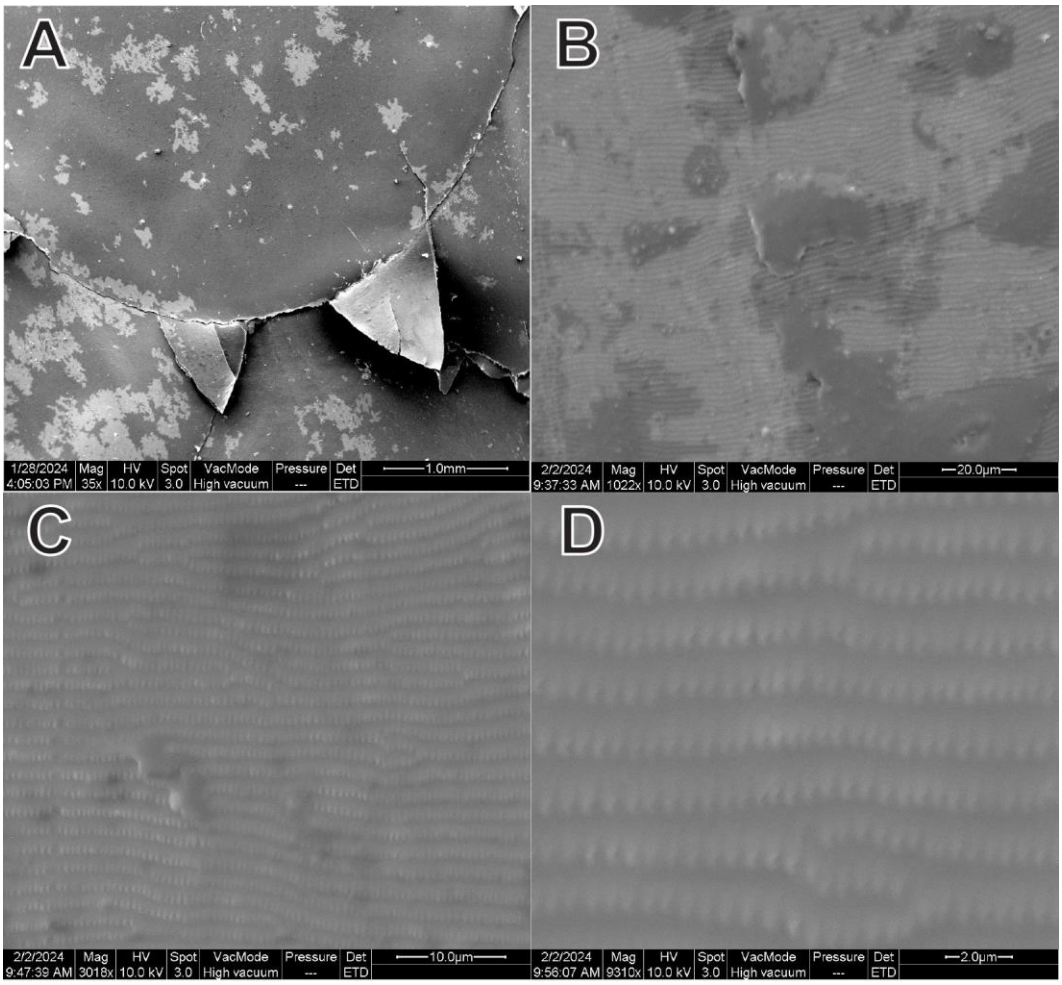

Xenopeltis unicolor • Xenopeltidae • Middle Dorsal Skin

Figure 49. Unedited SEM images of *Xenopeltis unicolor* middle dorsal snakeskin microstructures. (A) Scale morphology (B-D) Scale microstructures at various levels of magnification

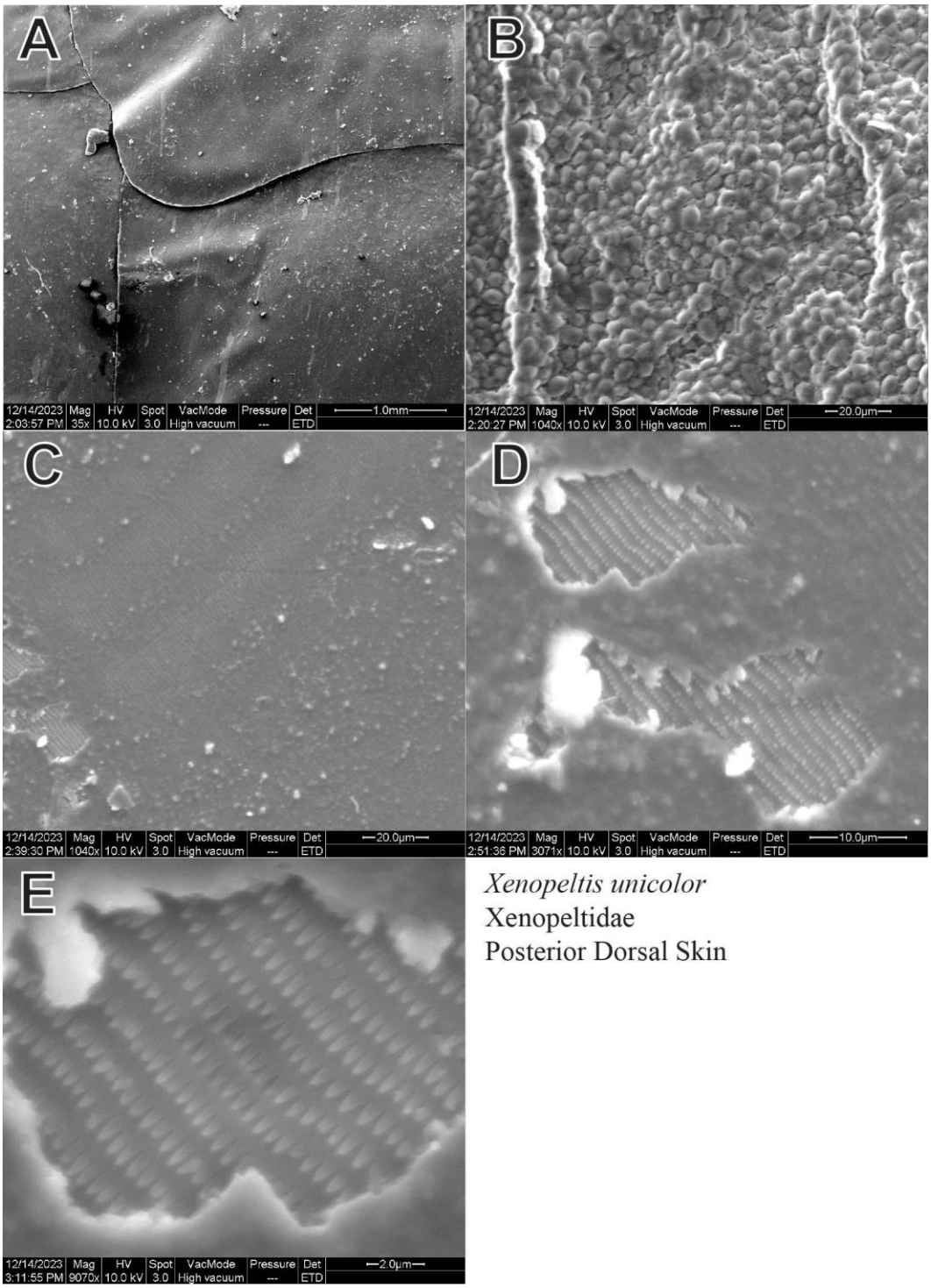

Figure 50. Unedited SEM images of *Xenopeltis unicolor* posterior dorsal snakeskin microstructures. (A) Scale morphology (B) Inter-scale keratinocytes (C-E) Scale microstructures at various levels of magnification

LITERATURE CITED

Alexander, N. J. Comparison of α and β keratin in reptiles. *Z. Zellforsch.* **110**, 153–165 (1970).

Alibardi, L. Adaptation to the land: The skin of reptiles in comparison to that of amphibians and endotherm amniotes. *Journal of Experimental Zoology Part B: Molecular and Developmental Evolution* **298B**, 12–41 (2003).

Allam, A. A. & Abo-Eleneen, R. E. Scales Microstructure of Snakes from the Egyptian Area. *jzoo* **29**, 770–775 (2012).

Arnold, E. n. History and function of scale microornamentation in lacertid lizards. *Journal of Morphology* **252**, 145–169 (2002).

Arrigo, M. I. *et al.* Phylogenetic mapping of scale nanostructure diversity in snakes. *BMC Evolutionary Biology* **19**, 91 (2019).

Branch, B. (William R.). *Field Guide to Snakes and Other Reptiles of Southern Africa*. (Sanibel Island, Fla. : Ralph Curtis Books, 1998).

Chiasson, R. B. The Apical Pits of Agkistrodon (Reptilia: Serpentes). *Journal of the Arizona-Nevada Academy of Science* **16**, 69–73 (1981).

Chiasson, R. B. & Lowe, C. H. Ultrastructural Scale Patterns in Nerodia and Thamnophis. *Journal of Herpetology* **23**, 109–118 (1989).

Cole, C. J. & Van Devender, T. R. Surface Structure of Fossil and Recent Epidermal Scales from North American Lizards of the Genus Sceloporus (Reptilia, Iguanidae). **156**, 451–514 (1976).

Das, I. *A Field Guide to the Reptiles of South-East Asia: Myanmar, Thailand, Laos, Cambodia, Vietnam, Peninsular Malaysia, Singapore, Sumatra, Borneo, Java, Bali*. (Bloomsbury Publishing PLc, 2015).

de Pury, S. Analysis of the Rubbing Behaviour of Psammophiids: A Methodological Approach. (Rheinische Friedrich-Wilhelms-Universität Bonn, 2011).

Dhillon, D. S. *et al.* Interactive Diffraction from Biological Nanostructures. *Computer Graphics Forum* **33**, 177–188 (2014).

Gans, C. & Baic, D. Regional Specialization of Reptilian Scale Surfaces: Relation of Texture and Biologic Role. *Science* **195**, 1348–1350 (1977).

Gillilland, M. Nerodia sipedon (Northern Water Snake). *Animal Diversity Web* https://animaldiversity.org/accounts/Nerodia_sipedon/ (2013).

Gower, D. J. Scale microornamentation of uropeltid snakes. *Journal of Morphology* **258**, 249–268 (2003).

Graf, A. Python regius (Ball Python, Royal Python). *Animal Diversity Web* https://animaldiversity.org/accounts/Python_regius/ (2011).

Harvey, M. B. Microstructure, ontogeny, and evolution of scale surfaces in xenosaurid lizards. *Journal of Morphology* **216**, 161–177 (1993).

Hazel, J., Stone, M., Grace, M. S. & Tsukruk, V. V. Nanoscale design of snake skin for reptation locomotions via friction anisotropy. *Journal of Biomechanics* **32**, 477–484 (1999).

Hillman, M. Morelia viridis (Green tree python). *Animal Diversity Web* https://animaldiversity.org/accounts/Morelia_viridis/ (2010).
Hoge, A. R. & Santos, P. S. Submicroscopic structure of stratum corneum of snakes. *Science* **118**, 410–411 (1953).
Horstmann, E. Elektronenmikroskopische Untersuchungen an der Epidermis von Reptilien. *Anat. Anz.* **113**, 87–93 (1964).
Irish, F., Williams, E. & Seling, E. Scanning electron microscopy of changes in epidermal structure occurring during the shedding cycle in squamate reptiles. *Journal of Morphology* **197**, 105–126 (1988).
Jackrel, S. Regina alleni (Striped Crayfish Snake). *Animal Diversity Web* https://animaldiversity.org/accounts/Regina_alleni/ (2012).
Leydig, F. *Ueber Organe eines sechsten Sinnes: zugleich als Beitrag zur Kenntniss des feineren Baues der Haut bei Amphibien und Reptilien*. (Druck v. E. Blochmann & Sohn, 1868).
Leydig, F. Ueber die äusseren Bedeckungen der Reptilien und Amphibien. *Archiv f. mikrosk. Anatomie* **9**, 753–794 (1873).
Maderson, P. F. A. The skin of lizards and snakes. *J. Herpet* **3**, 151–154 (1964).
Mattison, C. *Snakes*. (HarperCollins Publishers, 2008).
Mobasseri, S. *et al.* Patterning of human epidermal stem cells on undulating elastomer substrates reflects differences in cell stiffness. *Acta Biomaterialia* **87**, (2019).
Picado, C. Epidermal microornaments of the Crotalinae. *Bull. Antivenin Inst. Am* **4**, 104–105 (1931).
Pockrandt, D. Beiträge zur Histologie der Schlangenhaut. *Zool. Jahrb.* **62**, 275–322 (1937).
Price, R. Microdermatoglyphics: The Liodytes-Regina Problem. *Journal of Herpetology* **17**, 292–294 (1983).
Price, R. & Kelly, P. Microdermatoglyphics: Basal Patterns and Transition Zones. *Journal of Herpetology* **23**, 244–261 (1989).
Price, R. M. Dorsal Snake Scale Microdermatoglyphics: Ecological Indicator or Taxonomic Tool? *Journal of Herpetology* **16**, 294–306 (1982).
Rasmussen, L. Pituophis melanoleucus (Eastern Pine Snake). *Animal Diversity Web* https://animaldiversity.org/accounts/Pituophis_melanoleucus/ (2012).
Rutland, C. S. *et al.* Reptilian Skin and Its Special Histological Structures. in *Veterinary Anatomy and Physiology* (IntechOpen, 2019). doi:10.5772/intechopen.84212.
Sacha, M., Weisbach, N., Pöhler, A.-S., Demmerle, N. & Haltner, E. Comparisons of the Histological Morphology and In Vitro Percutaneous Absorption of Caffeine in Shed Snake Skin and Human Skin. *Slovenian Veterinary Research* **57**, (2020).
Schindelin, J. *et al.* Fiji: an open-source platform for biological-image analysis. *Nat Methods* **9**, 676–682 (2012).
Schmidt, C. V. & Gorb, S. N. *Snake Scale Microstructure:* vol. 157 (Schweizerbart Science Publishers, Stuttgart, Germany, 2012).

Schoch, C. L. *et al.* NCBI Taxonomy: a comprehensive update on curation, resources and tools. *Database (Oxford)* **2020**, baaa062 (2020).
Spinner, M., Kovalev, A., Gorb, S. N. & Westhoff, G. Snake velvet black: hierarchical micro- and nanostructure enhances dark colouration in Bitis rhinoceros. *Sci Rep* **3**, 1846 (2013).
Wall, F. *Ophidia Taprobanica; or, The Snakes of Ceylon*. (Colombo, H. R. Cottle,
govt. printer, 1921).